Research Square

Preprints are preliminary reports that have not undergone peer review.
They should not be considered conclusive, used to inform clinical practice,
or referenced by the media as validated information.

Numerical Investigation on P-Y Method of Group Piles under Static and Dynamic Loads

Mehmet ömer Timurağaoğlu (omertao@gmail.com)
Uludag University: Bursa Uludag Universitesi https://orcid.org/0000-0002-6329-905X
Yasin Fahjan
Istanbul Technical University: Istanbul Teknik Universitesi
Adem Doğangün
Uludag University: Bursa Uludag Universitesi

Research Article

Keywords: P-Y method, Finite element analysis, Static, Dynamic, P-multiplier, Nonlinear

Posted Date: June 17th, 2022

DOI: https://doi.org/10.21203/rs.3.rs-1719303/v1

License: This work is licensed under a Creative Commons Attribution 4.0 International License.
Read Full License

Numerical Investigation on P-Y Method of Group Piles under Static and Dynamic Loads

Abstract

The present study aims at scrutinizing the static and dynamic behavior of pile-soil interaction in the context of p-y method using finite element analysis. For this purpose, a series of static and dynamic analyses are carried out for single pile, 2x2 and 3x3 group piles in homogeneous clayey soil. In the analysis, the nonlinear behavior of soil is taken into account using a kinematic hardening model, while piles are modeled as elastic. The soil model parameters are calibrated using experimental modulus degradation and damping curves. The pile-soil interface is modeled considering normal and shear behavior to account for separation and sliding between soil and pile elements. In the static analyses, variation of pile moments and displacements with depth and the back-calculated p-y curves are evaluated. The soil resistance is directly obtained by extracting the shear and normal forces of the nodes in a pile at any depth. The p-multipliers for 2x2 and 3x3 group piles are calculated and compared with that of the experiments. The variation of p-multipliers with depth and lateral displacement is also evaluated. In dynamic analyses, first, site response analyses are carried out and validated against one-dimensional results under different loading frequencies. Infinite elements are applied at the boundaries to provide non-reflective boundaries. Later, single, 2x2 and 3x3 group pile analyses are executed. The influence of loading amplitude and frequency on the response are investigated using moment-depth and displacement-depth relationships. Dynamic p-y curves are back-calculated and the results are deeply assessed by comparing with static curves.

Keywords: P-Y method; Finite element analysis; Static; Dynamic; P-multiplier; Nonlinear

1. Introduction

In parallel with the developments in industry and technology in the last century, the diversity of buildings has increased to meet the needs. New building types (high buildings, viaducts, bridges, etc.) are built in city centers for prestige purposes, usually to meet commercial demands. These unique structures today are not only indicators of power and prestige but also the pinnacle of engineering. In the selection of foundations of such structures, piled systems, which are a type of deep foundation, are preferred instead of shallow foundations due to reasons such as increased loads from the structure, weak soil, or material losses. On the other hand, earthquake effects should also be considered in the design of engineering structures built in regions where seismicity is intense.

The P-Y method (Matlock 1970), which is proposed to represent the nonlinear interaction between the pile and the soil, is frequently preferred in pile-soil interaction problems. The method is later developed for different soil types (Welch and Reese 1972; Reese et al. 1974, 1975; Reese and Welch 1975). In these experimental studies, the behavior of piles in offshore structures under static and cyclic loads is examined and the process steps are suggested to obtain P-Y curve sets for different soil types. However, these studies' most important and common deficiency is that they are recommended for single piles under static or reversible (repetitive, cyclic) loads. As a matter of fact, piles are generally designed and analyzed as a group and exposed to earthquake effects.

Firstly, Brown et al. (Brown et al. 1988b) compared the behavior of piles in group piles under static lateral loads with that of a single pile. In this study, it was concluded that the behavior of the piles in the back rows is quite different from that of the single pile due to the shadowing effect. In the same study, P-multiplier values were suggested for each row of piles in the direction of loading. This value is expressed as the ratio of the load on each pile in the group to the single pile. In the following years, extensive studies were carried out on this subject. Similar to the first studies, the behavior under static and cyclic loads was examined in these studies. McVay et al. (McVay et al. 1998) investigated pile group interaction effects in loose and medium dense sand. Based on the test results, they found that p-multiplier are independent of soil density and only a function of the pile group geometry. Rollins et al. (Rollins et al. 1998) performed a full-scale pile group under static lateral loads to determine pile-soil-pile interaction effects. Compared with the single pile behavior, they found out that shadowing/group effects significantly reduced load capacity for all rows. A series of centrifuge tests are conducted to scrutinize laterally loaded pile groups in normally and over consolidated clays by Ilyas et al. (Ilyas et al. 2004). Unlike other studies, they employed the individual performance of piles in the group. They concluded that the simplification of studying with the average performance of piles in the same row rather than the performance of individual piles is acceptable for lead and rear row but center piles in the middle rows carry much less loads than outer piles. Also, different equations have been proposed in the literature to determine the p-multipliers (Rollins et al. 2003; AASHTO 2017; TBEC 2018; Reese et al. 2019) depending on pile interval and geometry/row position.

There are also several 3D numerical studies on the p-y method in the literature (Yang and Jeremic 2003; Kim and Jeong 2011; Lu and Zhang 2020; Xiao-ling et al. 2020; Timurağaoğlu et al. 2021). Rahmani et al. (Rahmani et al. 2018) evaluated static and dynamic P-Y curves under lateral loading by comparing them with API (API 2007)

curves. They indicated that API springs could not capture the mechanism in soil-pile interaction, although they are more often applied in design. By performing 3D finite element analysis to develop p-multipliers for fixed and free headed 3×3 to 5×5 vertically squared pile groups, Muhammed et al. (Adeel et al. 2020) found out that, for fixed-head pile groups, p-multipliers are lower because of higher group interactions compared with the free-head pile groups.

However, the literature on the behavior of piles under dynamic loads is limited. Considering two different single pile arrangements in a profile of soft clay overlying dense sand, Boulanger et al. (1999) investigated the dynamic P-Y method under various shaking amplitudes. The dynamic P-Y analyses were able to model the recorded responses reasonably. Ting et al. (Ting et al. 1987) stated that the secant slope of the dynamic P-Y curve is highly dependent on the loading frequencies in dynamic pile load tests. El Naggar and Bentley (El Naggar and Bentley 2000) observed that the soil resistance increases under dynamic loading due to the damping effect. They also stated that the dynamic P-Y curves depend on the loading frequency. In two different experimental studies (Yang et al. 2011; Lim and Jeong 2018) on the behavior of single piles under dynamic loads, it is stated that dynamic P-Y curves give very different responses than static curves and the parameters affecting the response are determined by the acceleration amplitude and frequency given to the system (Yang et al. 2011; Lim and Jeong 2018), relative stiffness (Lim and Jeong 2018), pile bending stiffness and mass at the pile end (Yang et al. 2011). However, no experimental study focusing on the P-Y method has been found in the literature on the behavior of group piles under dynamic loads. Especially in group piles under dynamic loads, the need to determine the parameters affecting the P-Y method arises.

This study examines the dynamic P-Y curves in group piles and the loading amplitude and frequency affecting these curves using three-dimensional (3D) numerical models. For this purpose, 3 static and 27 dynamic analyses are conducted for single pile, 2x2 and 3x3 group piles. The results are evaluated in terms of moment-depth, displacement-depth and p-y curves. P-multipliers are assessed by comparing with experimental results available in the literature. The variation of P-multipliers with lateral displacement and depth is also scrutinized. Static and dynamic p-y curves are generated and results are compared to assess the load sharing mechanism between each row and individual pile.

2. Generation of Numerical Model

2.1. Soil constitutive model

A yield surface, a hardening and a flow rule to overcome limitations of the deformation theory of plasticity generally describe a constitutive model that can most accurately represent complicated soil behavior. Yield surface estimates whether the material should behave elastic or plastic under a load increment. The hardening rule governs the shape of the stress-strain curve due to plastic straining. The flow rule defines the direction of the plastic strain increment. It is well known that models with isotropic hardening rules generally apply to monotonic loading. In contrast, kinematic or mixed hardening models are more appropriate for cyclic or Bauschinger effects (Chen and Mizuno 1990). For the above considerations, an advanced constitutive soil model is selected for utilization in nonlinear dynamic analysis. This model is first proposed to simulate the cyclic response of shallow foundations (Anastasopoulos et al. 2011). Later, it is implemented in several different areas (Gerolymos et al. 2005; Giannakos et al. 2012; Kampitsis et al. 2015; Mucciacciaro and Sica 2018). The detailed information of KH model is available in mentioned papers and program documentation (Abaqus 2020).

2.2. Absorbing Boundary Conditions

Special/artificial boundary conditions should be provided for modeling purposes to absorb the waves at the boundaries, especially in the dynamic analysis of 3D models. These boundaries should be able to perfectly absorb all types of waves (body waves and surface waves) at all angles of incident and frequencies propagating outward. The infinite element available in Abaqus has been chosen as the boundary condition for the soil. These elements are placed at boundaries on four sides of the soil (two sides for 1-directional analysis). For infinite elements, only the elastic material needs to be defined (Abaqus 2020). Infinite elements provide the "silent" (non-reflective) boundary condition to the finite element model with a damping matrix effect, but do not contribute to the stiffness matrix of the finite element. Infinite elements contribute nothing to the intrinsic modes of the system. These elements are used for the far-field region of the static (Zienkiewicz et al. 1983) and dynamic (Lysmer and Kuhlemayer 1969) response. Infinite elements are successfully applied in literature (Nguyen et al. 2017; Fatahi et al. 2018)

2.3. Soil-pile Interaction

When the surfaces are in contact, they generally transmit shear forces and normal forces between the interfaces. These two force components form the basis of the piles' horizontal and vertical load transfer mechanism. The representation of pile-soil interaction is important in modeling piled systems using the finite element method. In the pile-soil interaction, separation, coupling and friction behavior must be accurately defined. This behavior can be represented numerically by defining normal and frictional behavior at the interface of soil and pile.

Abaqus provides its users with a variety of contact formulations. Each formulation is based on a Contact Discretization, a Tracking Approach, and the assignment of "master" and "slave" roles to contact surfaces. In addition, the pressure-penetration relationship and constraint enforcement method needs to be defined.

For the contact discretization, the surface to surface formulation is adopted to provide the contact conditions on an average sense not only at the slave nodes, but also close to these nodes. In the tracking approach, there are two types; One is the finite sliding, which is the most general and allows any random movement of the surfaces, and the other is the small sliding, which assumes that even though the two bodies undergo large movements, there will be relatively little slip of one surface along the other. The finite sliding approach is the most general tracking approach and was chosen because it allows for random relative separation, sliding and rotation of the contacting surfaces. In assigning a master-slave role, when both surfaces in the contact pair are element-based and attached to the deformable masses or the deformable mass is defined as rigid, slave and master surfaces must be chosen. This selection is essential for node-to-surface contact. In general, if a smaller surface is in contact with a larger surface, it is optimal to select the smaller surface as the slave surface. If this distinction cannot be made, the main surface should be chosen as the surface of the more rigid mass, or if the two surfaces have comparable stiffnesses, the mass with the coarser mesh should be selected as the master surface.

When defining the pressure-overclosure relationship, using the hard contact minimizes the penetration of the slave surfaces to the master surface at the constraint regions. It does not allow the transfer of tensile stress across the interface. When the surfaces come into contact, any contact pressure can be transmitted between them. The surfaces are separated when the contact pressure drops to zero. The separated surfaces come into contact again when the gap between them drops to zero (Figure 1a). However, over-constraining problems have emerged in the analysis when this relationship is applied. To overcome this problem, the penalty method is used in the study. This method is a stiff approximation of hard contact. The method attempts to predict the hard pressure-penetration

behavior. In this method, the contact force is proportional to the penetration distance so that some penetration will occur (Figure 1a).

On the other hand, the relationship known as friction between contacting bodies is usually expressed in terms of stresses at the interface of the bodies. The friction models available in the Abaqus program include the classical Coulomb friction models. In general, the Coulomb model allows the coefficient of friction to be defined by slip rate, contact pressure, the average surface temperature at the contact point, and area variables. The basic friction model assumes that the coefficient of friction is the same in all directions (isotropic friction). For a three-dimensional simulation, there are two vertical components of shear stresses τ_1 and τ_2 along with the interface between two bodies. These components move in local tangential directions to the contact surfaces or contact elements. The model combines two shear stress components as "equivalent shear stress" ($\overline{\tau}$) for stick/slip calculations ($\overline{\tau} = \sqrt{\tau_1^2 + \tau_2^2}$). In addition, the two shear rate components are combined ($\dot{\gamma}_{eq}$) at an equivalent slip rate ($\dot{\gamma}_{eq} = \sqrt{\dot{\gamma}_1^2 + \dot{\gamma}_2^2}$). stick/slip calculations describe a surface where a point in the contact pressure-shear stress plane transforms from stick to slip (Figure 1b). The friction coefficient was accepted as 0.5 in accordance with the recommended range in the literature (Mat Nor et al. 2015; Belinchon et al. 2016).

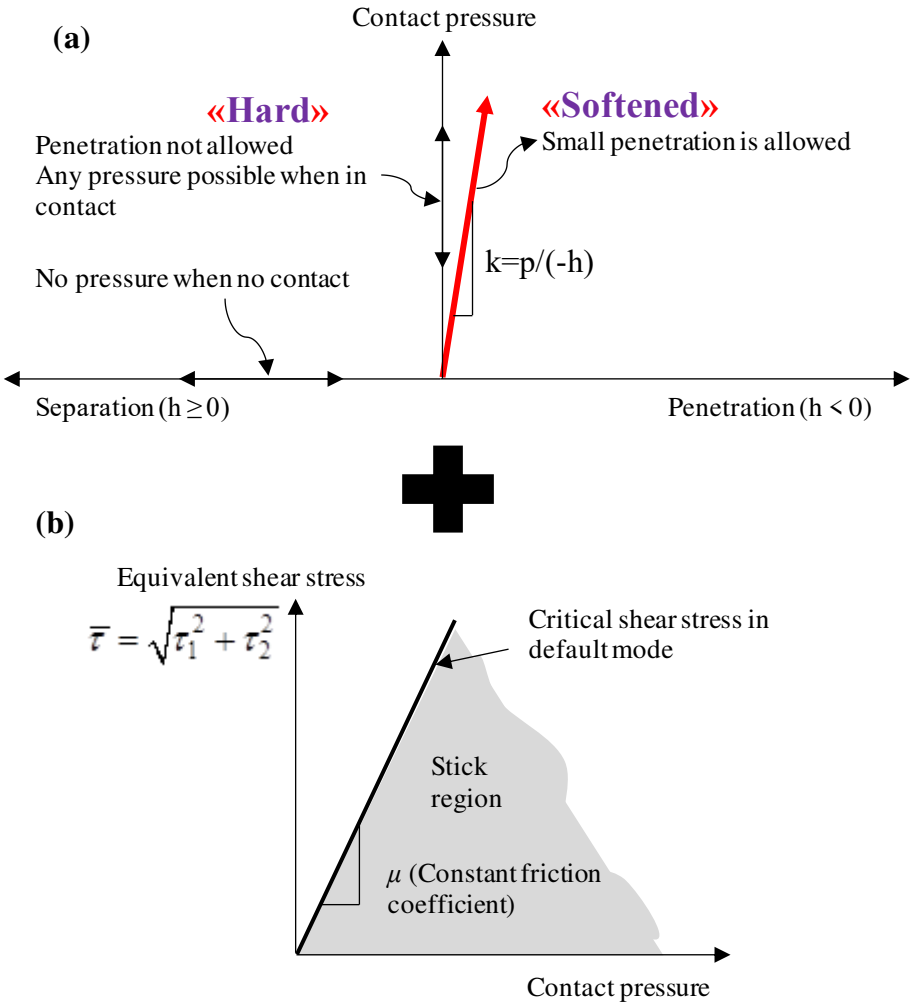


Figure 1. Definition of normal and tangential (frictional) behavior

2.4. Boundary conditions and loadings

The analyses are conducted in two separate steps for static and dynamic analysis. In the static analysis of the first step, the bottom of the system is fixed while sides are constrained in x and y directions and vertical motions are released. In the dynamic analysis of the first step, the bottom is fixed and the horizontal displacement is constrained in the direction perpendicular to the loading direction while infinite elements are placed to the boundaries in loading directions to avoid wave reflections. In the second step, loadings are applied to the system. The load is applied to the pile cap as a force in static analysis. However, in implicit dynamic analysis, the displacements at the bottom in the loading direction is released. The loading was applied from the bottom of the system in the form of a sine wave (asin($2\pi ft$)) with different amplitudes (0.1, 0.3 and 0.5g) and frequencies (1, 2 and 4 Hz). The time step for dynamic analysis is selected as 0.004 depending on the mesh size and frequency of loading as stated in

the literature (Jeremić et al. 2009). 8-node linear hexahedral solid elements with reduced integration (C3D8R) are used for both soil and pile. The reason we use a reduced integration element is that fu lly integrated elements don't hourglass, but can suffer from "locking" behavior. When a reduced integration element is utilized, the locking doesn't occur, but the element is not rigid enough in non-critical bending to model the soil. Additionally, since the integration point is located in the middle of this element type, small elements are needed to capture the stress concentration at the interface. Thus, a finer mesh is adopted in the vicinity of the pile, while the coarser mesh is used through the external boundaries. 8-node linear, one-way infinite (CIN3D8) elements are used for absorbing boundaries. Generated model, together with the boundary conditions, are given in Figs. 2 to 4.

2.5. Generated 3D FE model

The soil depth is selected as 30m. The pile diameter is 1m, which is the commonly used diameter. The pile is assumed to be reinforced concrete and modeled as elastic. The pile length is 15.2 m and the height of the cap is 1 m. In soil pile analysis, the distance between piles was chosen as three times the pile diameter (3D). In this study, a 0.2 m gap was left between the soil surface and the cap to neglect the influence of the pile cap. A schematic view of the 3x3 group pile model used in the analysis is given in Figure 2. In single pile analyses, the dimensions do not change; only one pile is used. Homogeneous clayey soil with a PI of 50% and a shear wave velocity of 100 m/s was preferred in the analyses. This type of soil is defined as a ZE class according to the Turkish Building Earthquake Code (TBEC 2018). While smaller element size was chosen in the regions close to the piles, larger elements were preferred towards the boundaries. The generated 3D models are seen in Figures 3 and 4 for single pile and 3x3 group piles systems.

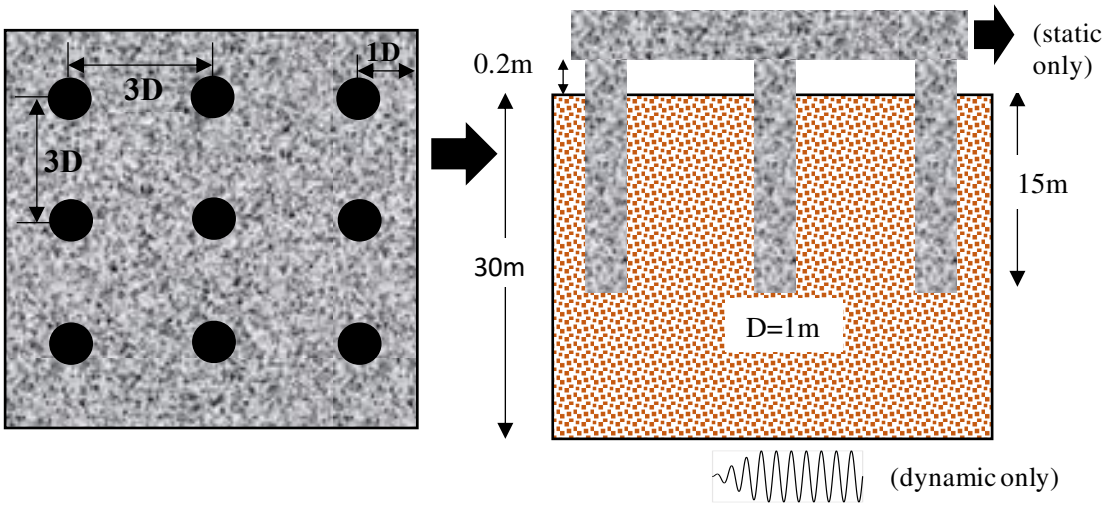


Figure 2. Schematic view of 3x3 group pile

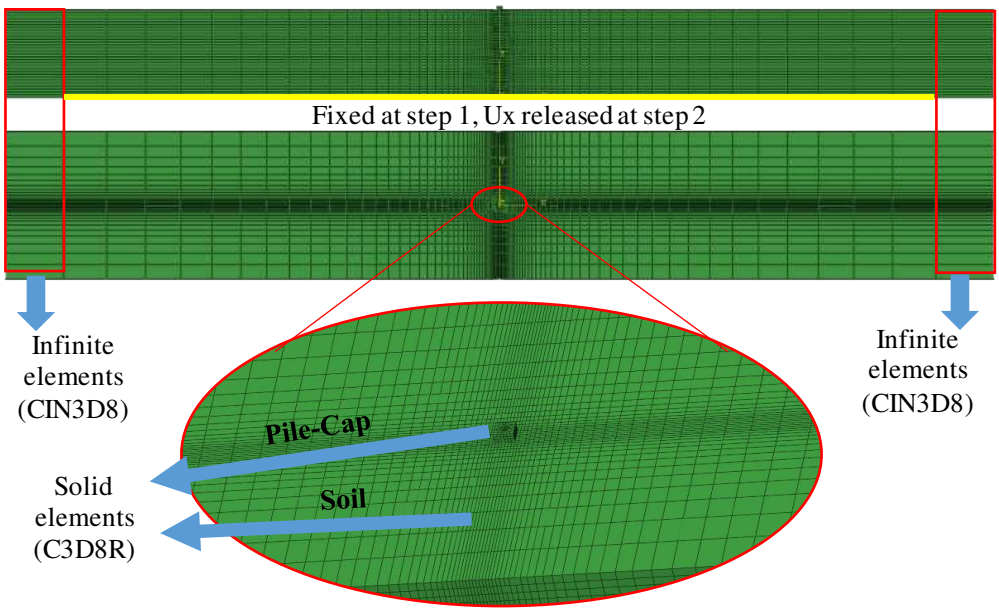


Figure 3. Generated 3D model of single pile

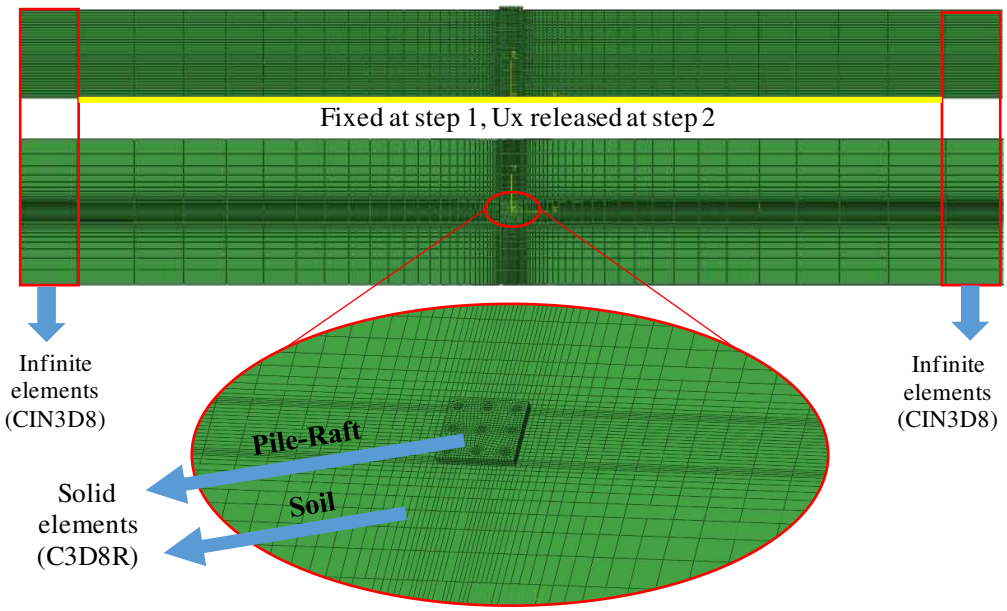


Figure 4. Generated 3D model of 3x3 group pile

3. Calibration of constitutive model parameters

Model parameters were numerically calibrated with the help of a strain-controlled simple shear test performed under cyclic loads (Figure 5). In these tests, calibration was performed for clay by considering the experimental G-γ and ξ-γ curve sets. It has been shown in the study that the plasticity index (PI) is one of the most effective parameters for many different soils (Vucetic and Dobry 1991). For this reason, PI-varying curve sets were used for clayey soils in this study. The results obtained from the cyclic simple shear test model for a plasticity index (PI) ratio of 50 % are illustrated in Figure 5, depending on shear strain magnitude. Numerical tests are implemented in Abaqus (Abaqus 2020) finite element computer program. The detailed calibration procedure of the model parameters is available in the literature (Anastasopoulos et al. 2011). The hysteretic damping ratio is typically calculated as illustrated in Figure 6.

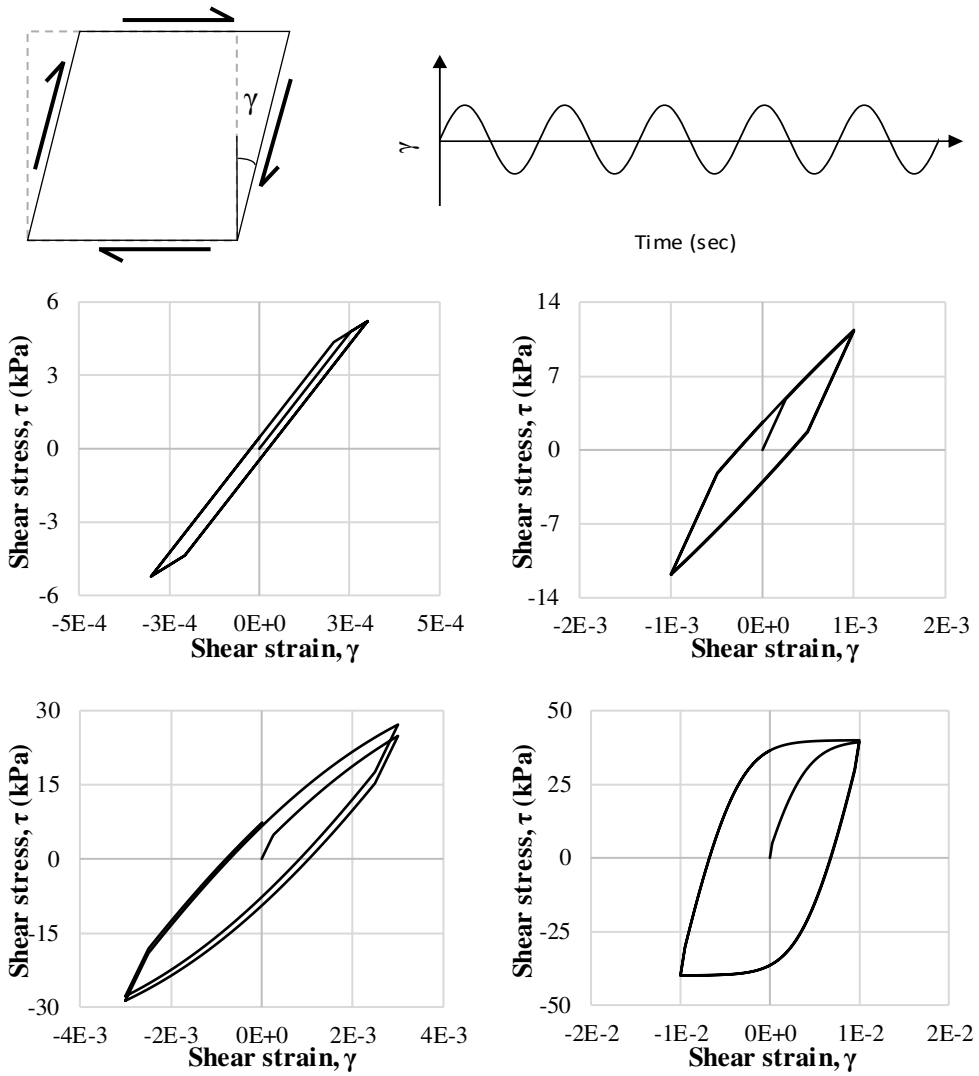


Figure 5. Numerical results of cyclic simple shear test for clay of PI = 50% (C_k=53 MPa, σ_0=8 MPa and γ_{kh}=870). Hysteretic loops for (a) γ =3E-4, (b) γ =1E-3, (c) γ =3E-3 and (d) γ =1E-2

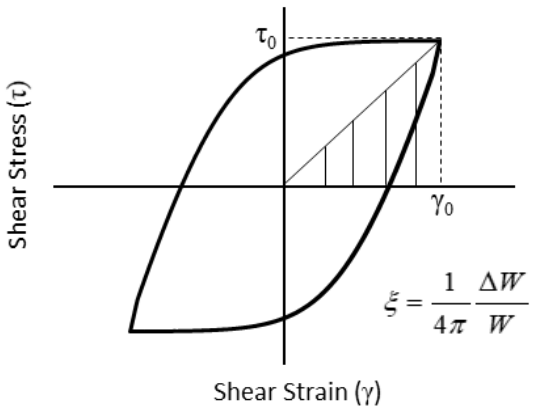


Figure 6. Typical shear stress-shear strain hysteresis loop for soil

After utilizing cyclic simple shear tests, one can calculate the change in shear modulus (G/G_{max}) and damping ratios (ξ) from shear stress-shear strain curves for various strain values. It is confirmed that PI is the main parameter governing G-γ and ξ-γ curves for various soils (Vucetic and Dobry 1991). After sensitivity analyses, a reasonable agreement with the G-γ curve is captured. The computed and experimental curves are compared for modulus degradation and damping ratios in Figure 7. Numerical results suit the experimental curve of PI=50% clay soil in the modulus degradation curve, whereas a reasonable agreement is encountered in the hysteretic damping curve. The parameters obtained after the calibration procedure are given in Table 1.

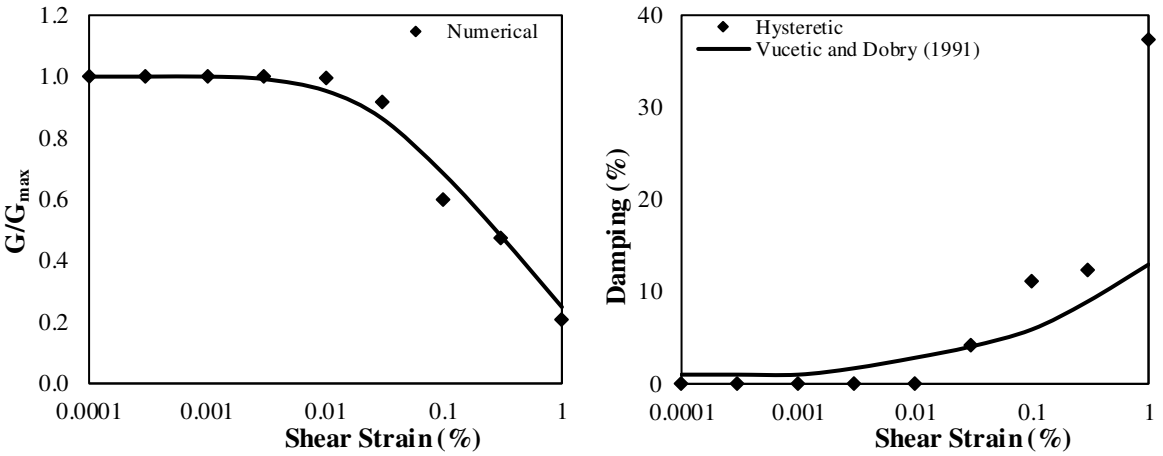


Figure 7. Calibrated soil model for Clay (PI = 50%, V_s = 100 m/s), comparison of numerical analysis and experimental test results for G-γ (left) and ξ-γ (right) curves.

Table 1. Adopted soil model parameters for clay

Soil type	V_s (m/s)	γ (kg/m^3)	υ	C_k (MPa)	PI (%)	S_u (kPa)	σ_0 (kPa)	γ_{kh}
Clay	100	1900	0.4	53	50	40	8	870

4. Numerical Analysis Results

4.1. Validation of 3D model

The first step of soil-structure interaction is site response analysis. (Wolf 1985). For this reason, site response analyses were carried out under different frequencies (2, 4, 6 and 8Hz). By changing the length/dimension of the

system, the response spectra of 3D model (Abaqus 2020) obtained on the ground surface were compared with the 1D Deepsoil (Hashash et al. 2017) results and the system length was decided. 1D and 3D elastic analysis results are given in Figure 8. Here, while compatible responses are obtained for 1D and 3D analyses at some frequencies for 200m length, it is understood that there are significant differences in the results at frequencies close to the resonance frequency. When the figures are examined, it is seen that the largest reactions occur at a frequency of 2 Hz. Undoubtedly, the resonant frequency is close to this value. When the results obtained by choosing different lengths in the system dimensions for this frequency are examined and considering the dimensions of the 3x3 group piles, 300m has been selected as the system length.

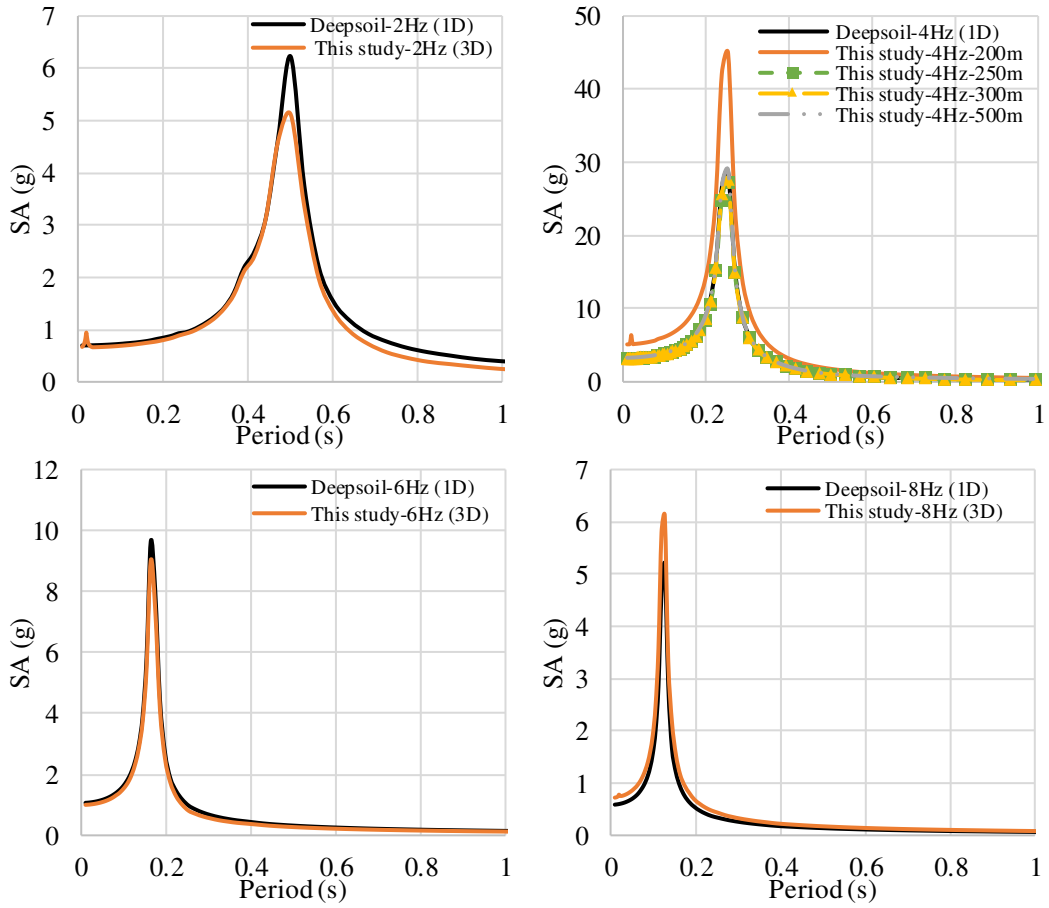


Figure 8. Comparison of response spectra at the ground surface for different frequencies

4.2. Static analysis results

Static analyses are conducted for single, 2x2 and 3x3 group piles to investigate the static p-multiplier parameter. Firstly, the shear stress-strain behavior of soil around the pile is given in Figure 9. The figure shows that the soil behavior around the pile is nonlinear. When the figure is examined, it is seen that the shear stress values increase as the number of group piles increases at the same strain levels. This increase is due to the shadowing effect (Brown et al. 1988b), as known in the literature.

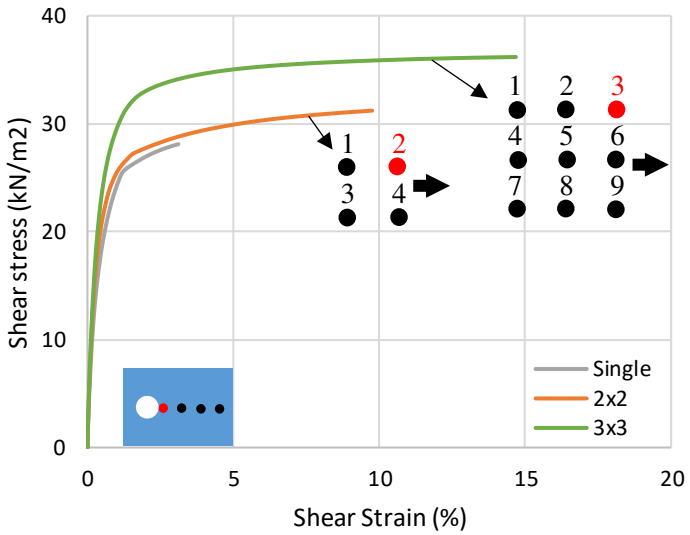


Figure 9. Comparison of shear stress-strain curves

The displacement-depth relationship of a single pile is compared with 2x2 and 3x3 group piles in Figure 10. It can be seen from the figures that the displacement behavior throughout the depth is different than single piles behavior for 2x2 and 3x3 group piles. The comparison of moment-depth relationships is given in Figure 11. The results are shown for the same displacement level of the pile cap. According to the result obtained from the figures, as the number of group piles increases, the depth at which the maximum moment and zero lateral displacements at the pile occur increases. According to the results of both 2x2 and 3x3 group piles, while the piles in the front rows carry more moment, the piles in the back rows carry less moment. The maximum moments for piles in the trailing rows occurred at greater depths, in line with the findings of Brown et al. (1988b).

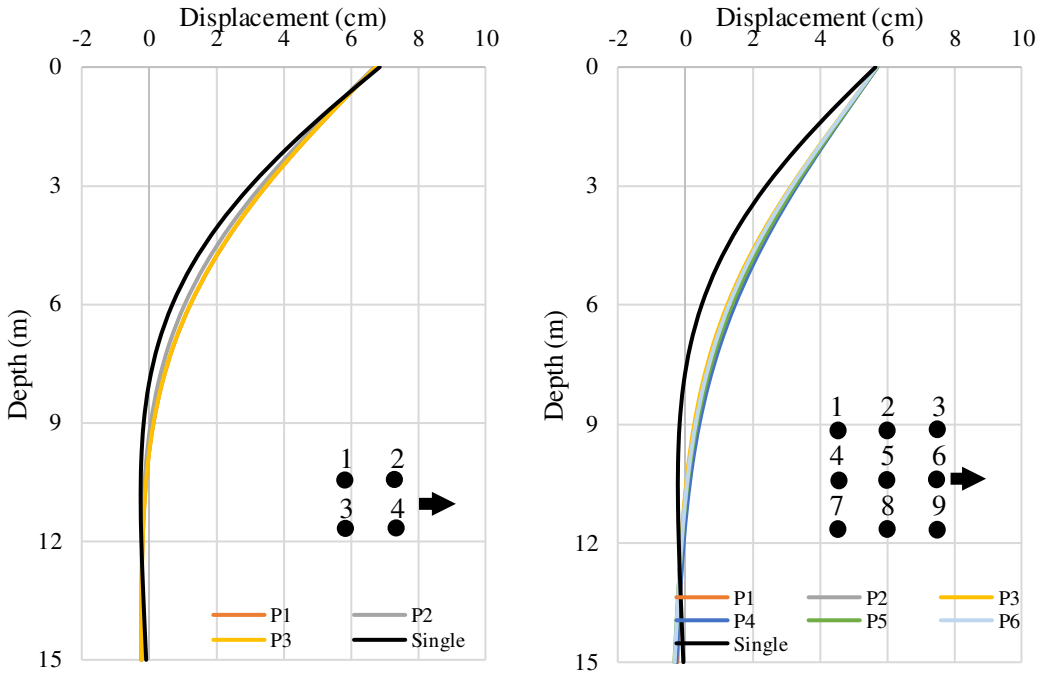


Figure 10. Comparison of displacement-depth relationships

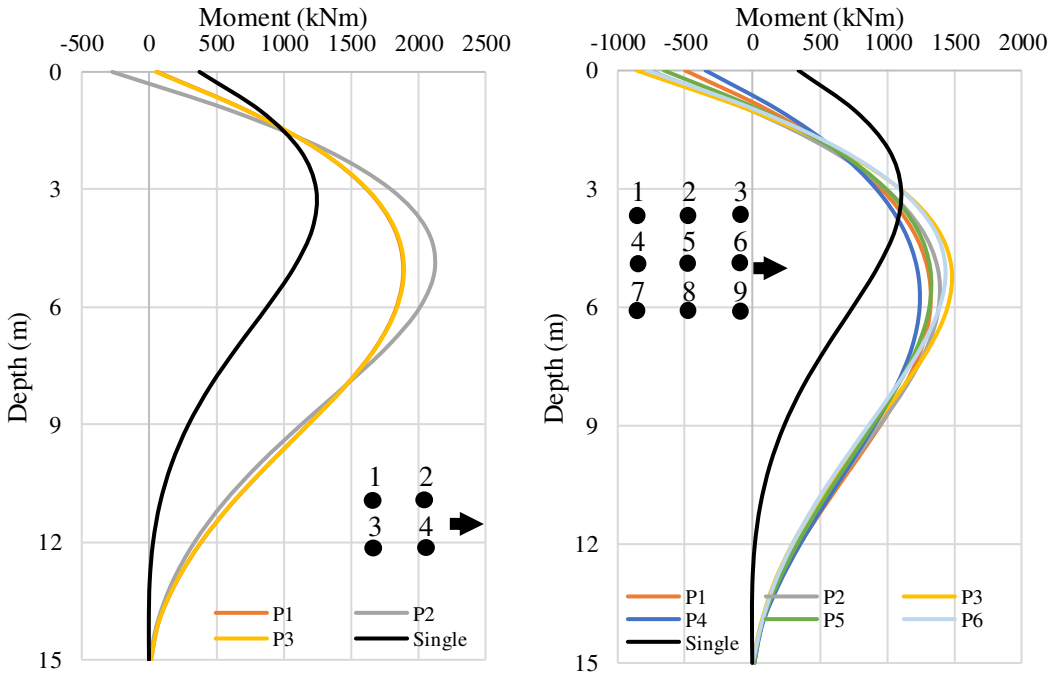


Figure 11. Comparison of moment-depth relationships

Soil resistance (p) and pile displacement are generally calculated as the second derivative of the moment profile of the pile according to simple beam theory (Yoo et al. 2013; Haouari and Bouafia 2020). However, this method is difficult to implement especially when the number of piles is increased and also, the results may alter when

derivation is not well utilized. On the other hand, the soil resistance can be obtained numerically by di viding the sum of the shear and normal forces of the nodes in a pile at any depth to the vertical mesh size as below:

$$P = \frac{\sum_{i=1}^{N} (CNORMF + CSHEARF)}{h} \tag{1}$$

where h is the vertical mesh size of the pile elements. Lateral displacement of pile (y) is directly obtained from the analysis results. The p-y curves at the first 3m depths of 2x2 group piles are compared with the results of single piles in Figure 12. In these figures, while pile 2 in the front row behaves closer to the single pile, the behaviors of piles 1 and 3 in the back row diverge from those of the single piles. These results are consistent with existing experimental studies in the literature (Rollins et al. 2003; Ilyas et al. 2004). However, although the behavior of the leading row piles is close to the behavior of the single pile at the ground surface, the behavior of all piles deviates from the behavior of the single pile as the depth increases. As expected, similar behavior is observed in piles 1 and 3 due to symmetrical boundary conditions and loadings.

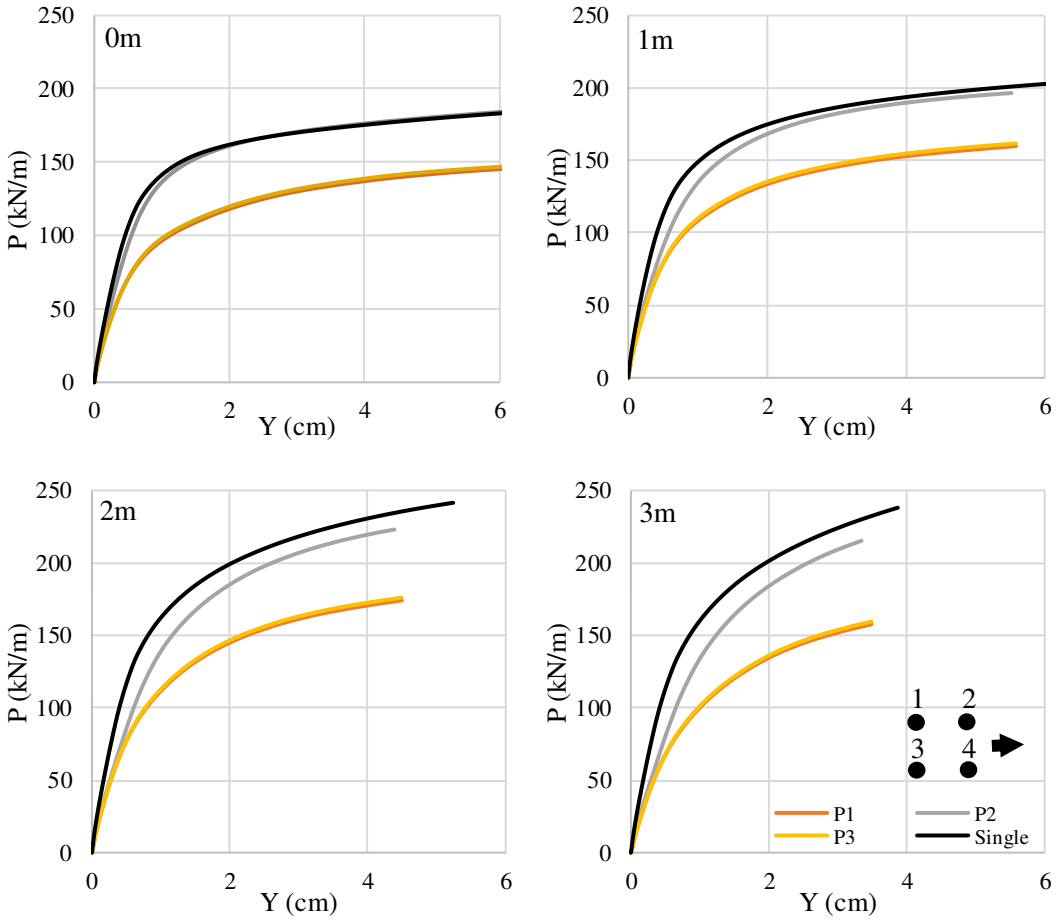


Figure 12. Comparison of p-y curves for different depths of 2x2 group piles

The p-y curves at the first 3m depths of 3x3 group piles are compared with the results of single piles in Figure 13. Similar to the results of 2x2 group piles, while the piles in the leading row take more load and behave closer to the single pile results, the piles in the middle and rear rows take less load and move away from the single pile behavior. Also, complex behavior is observed especially in 3x3 group piles at smaller displacement levels (approximately 1cm for this study). As the displacement increases, the loads on the piles become more pronounced and the behavior becomes easier to understand. Combining the maximum soil resistances across the depth, as shown in Figure 14, yields results similar to Figures 12 and 13. When this figure is examined, it is understood that the resistance of the single pile is higher than the resistance of each of the group piles for any depth.

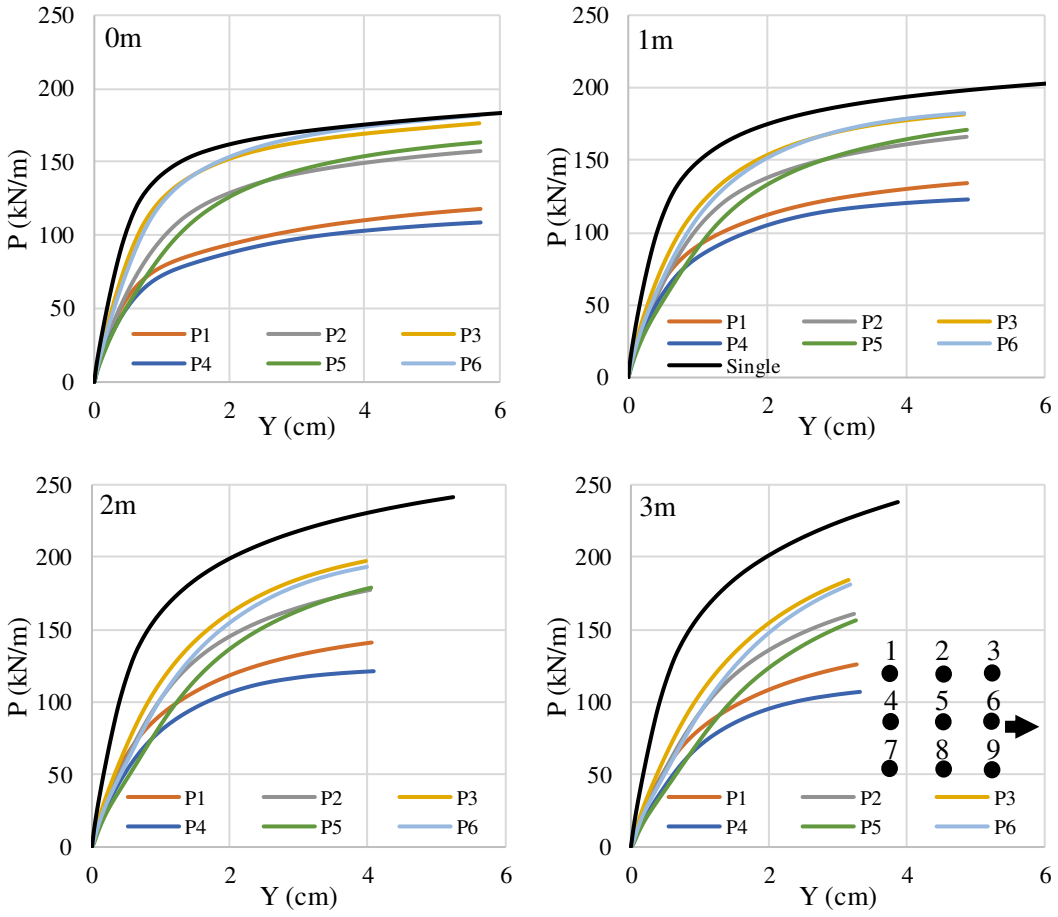


Figure 13. Comparison of p-y curves for different depths of 3x3 group piles

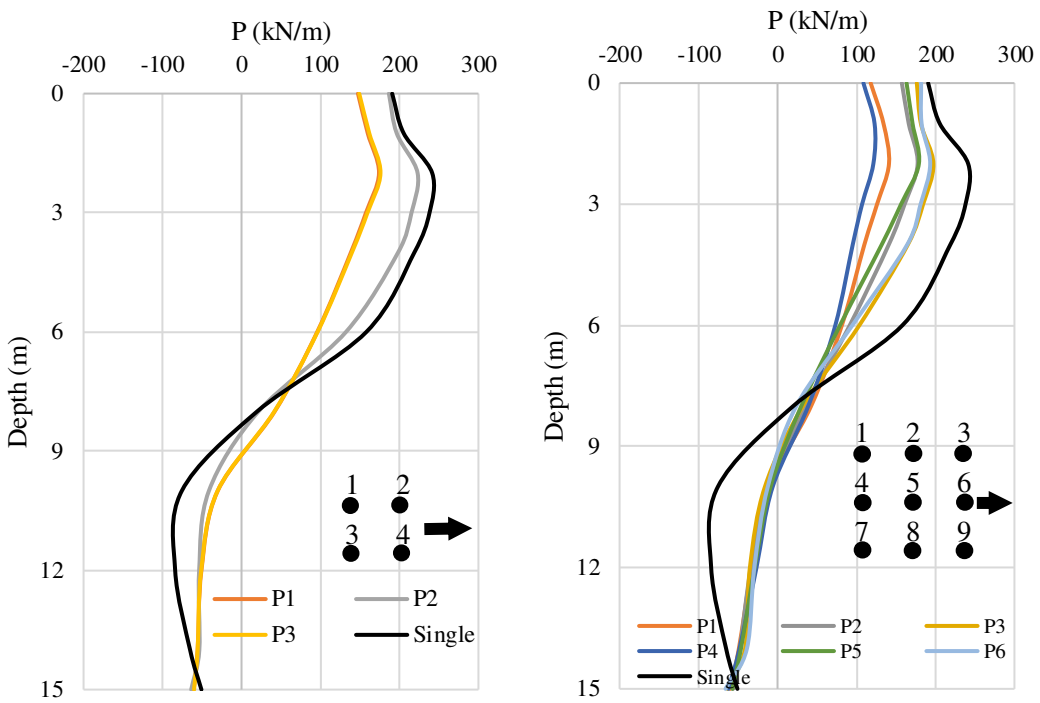


Figure 14. Comparison of maximum soil resistance across depth

Using the p-y curves from Figures 12 and 13 for 2x2 and 3x3 group piles, respectively, p-multipliers (Pm) are calculated. The calculated Pm values are compared with the existing literature for three rows as shown in Figure 15 and given in Table 2. The equation used in Figure 16 is also provided in Table 3. When the figure is examined, it is understood that the numerical p-multiplier values obtained under static loading in this study are compatible with the experimental studies in the literature. Additionally, within the scope of this study, the variation of the p-multiplier with the first 3m depth was also examined for 2x2 and 3x3 group piles as given in Figure 16. According to the results in the figure, the p-multiplier values generally have a decreasing trend.

Variations of p-multiplier with lateral displacement for 2x2 and 3x3 group piles are given in Figures 17 and 18, respectively. At low displacement levels, the p-multiplier value increases in the piles in the front and middle rows, while the p-multiplier starts to remain constant when the displacement increases. On the other hand, in the piles at the trailing rows, there is no significant change in the p-multiplier value while the displacement increases. Also, the increase rate becomes more pronounced as depth increases.

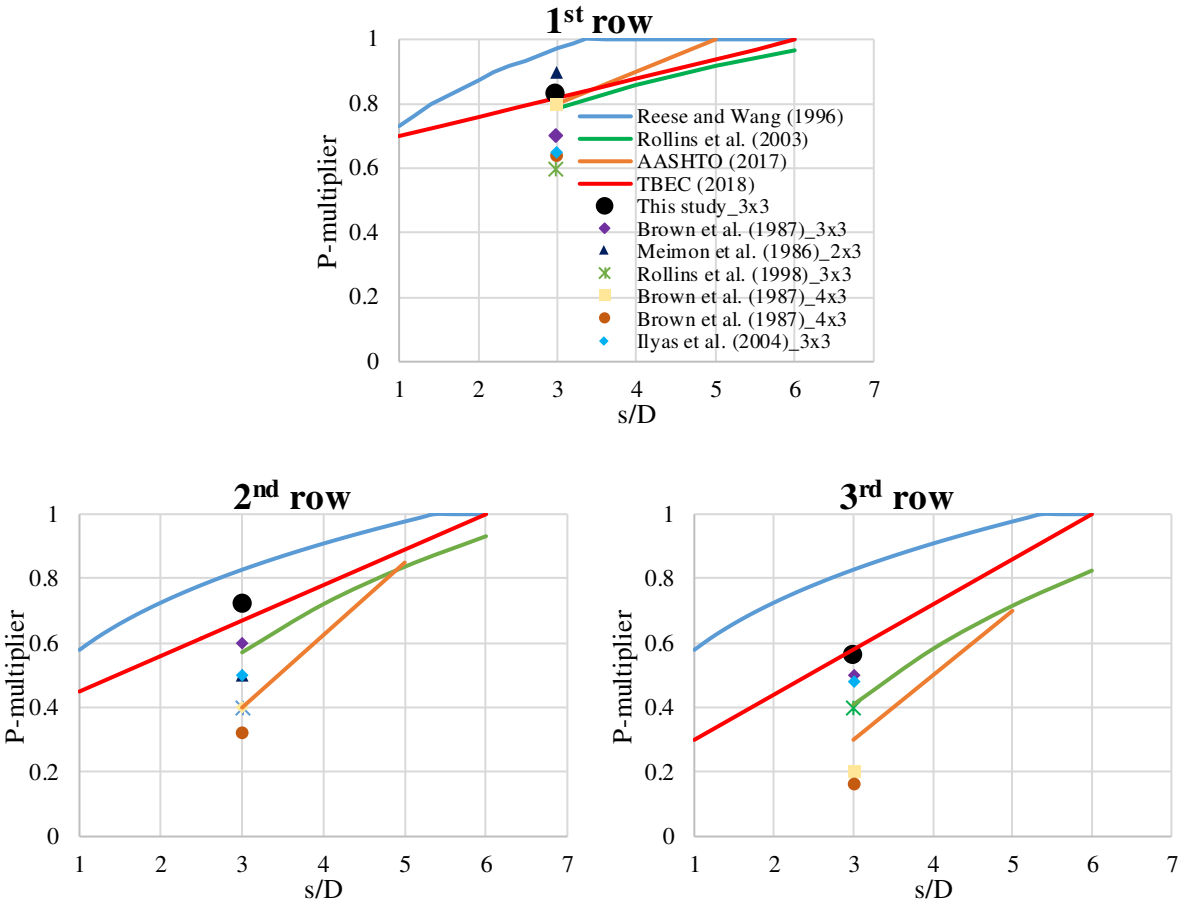


Figure 15. Comparison of p-multipliers according to rows

Table 2. P-multipliers suggested for clayey soils

Interval	Group	P-multiplier				Maximum Displacement	Reference	Head condition	Test type	Soil type
		1st row	2nd row	3rd row	4th row					
3	3x3	0.7	0.6	0.5		0.23d	Brown et al. (1988a)	Free	Full scale	Hard clay
3	2x3	0.9	0.5				Meimon et al. (1986)	Free	Full scale	Hard silty clay
3	3x3	0.6	0.4	0.4		0.19d	Rollins et al. (2003)	Free	Full scale	Clayey silt
3	4x3	0.8	0.4	0.2	0.3	0.51d	Brown et al. (1988a)	Fixed	Full scale	Soft clay
3	4x3	0.64	0.32	0.16	0.24	0.20d	Brown et al. (1988a)	Fixed-Free	Full scale	Sandy clay
3	3x3	0.65	0.5	0.48		0.5d	Ilyas et al. (2004)	Free	Centrifuge	Kaolin clay
3	4x4	0.65	0.49	0.42	0.46	0.5d	Ilyas et al. (2004)	Free t	Centrifuge	Kaolin clay
3	3x3	0.83	0.72	0.56		0.6d	This study	Fixed	Numerical	Clay
3	2x2	0.94	0.73			0.6d	This study	Fixed	Numerical	Clay

Table 3. References and equations used in Figures

Reference	Equation
Reese et al. (2019)- 1st row	If $1 \le s/d \le 5.37$; $0.5791(s/d)^{(0.3251)}$ If $s/d > 5.37$; 1.0
Reese et al. (2019)- Trailing rows	If $1 \le s/d \le 3.37$; $0.7309(s/d)^{(0.2579)}$ If $s/d > 3.37$; 1.0
Rollins et al. (2003)	1st row: $0.26\ln(s/d)+0.5$ 2nd row: $0.521\ln(s/d)$ 3rd row: $0.601\ln(s/d)-0.25$
TBEC (TBEC 2018)	$\beta_G = 0.2\left[(1-\beta_{G1})s-(1-6\beta_{G1})\right]$ where β_{G1}=0.7; 0.45; 0.3 and 0.2 for 1st, 2nd, 3rd, and 4th row
AASHTO (2017)	If s/d=3; 1st row=0.8; 2nd row=0.4; 3rd row=0.3 If s/d=5; 1st row=1; 2nd row=0.85; 3rd row=0.7

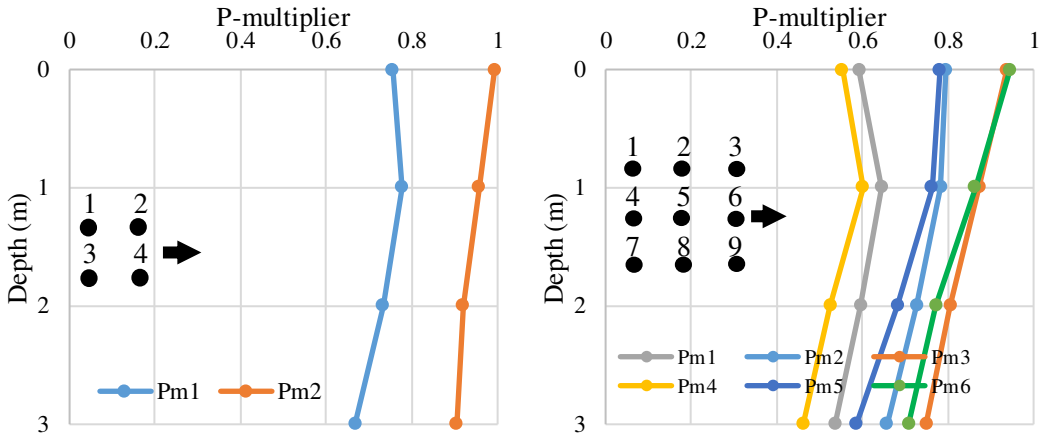


Figure 16. Variation of p-multipliers with depth (0-3m) for 2x2 and 3x3 pile group

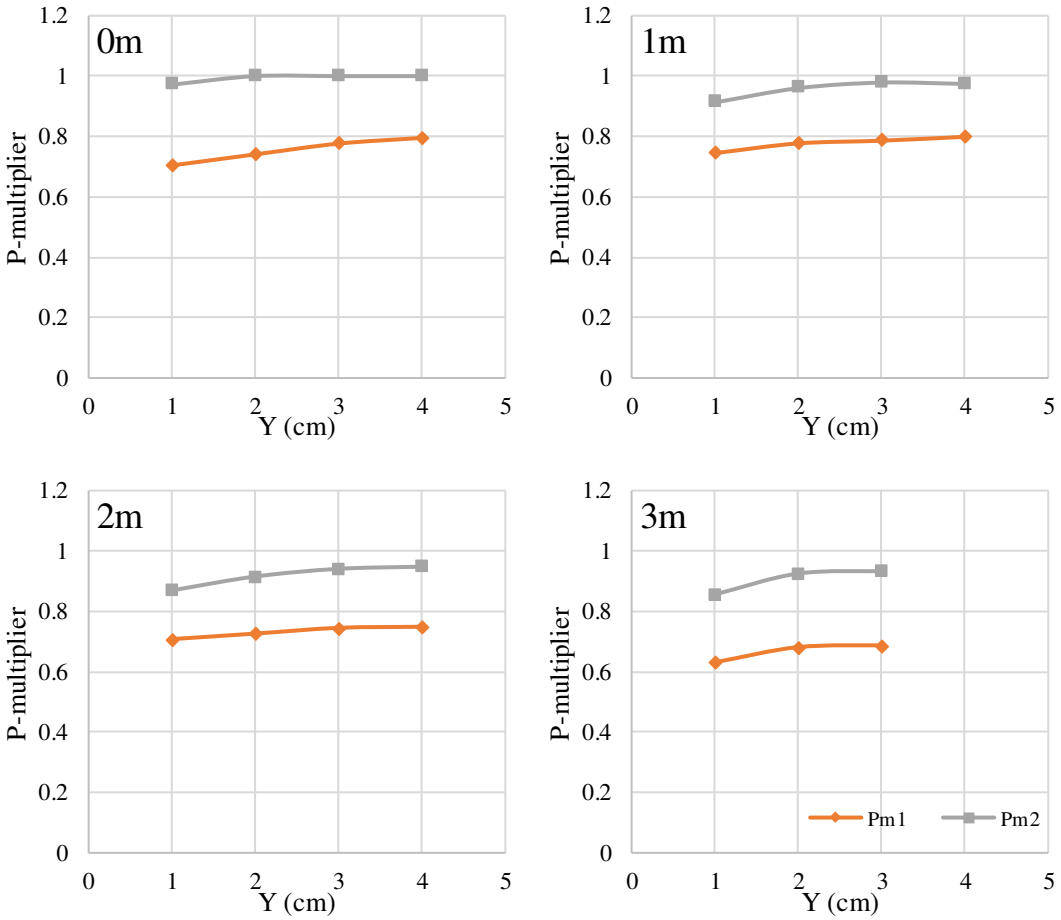


Figure 17. Variation of p-multipliers with lateral displacement for 2x2 pile group

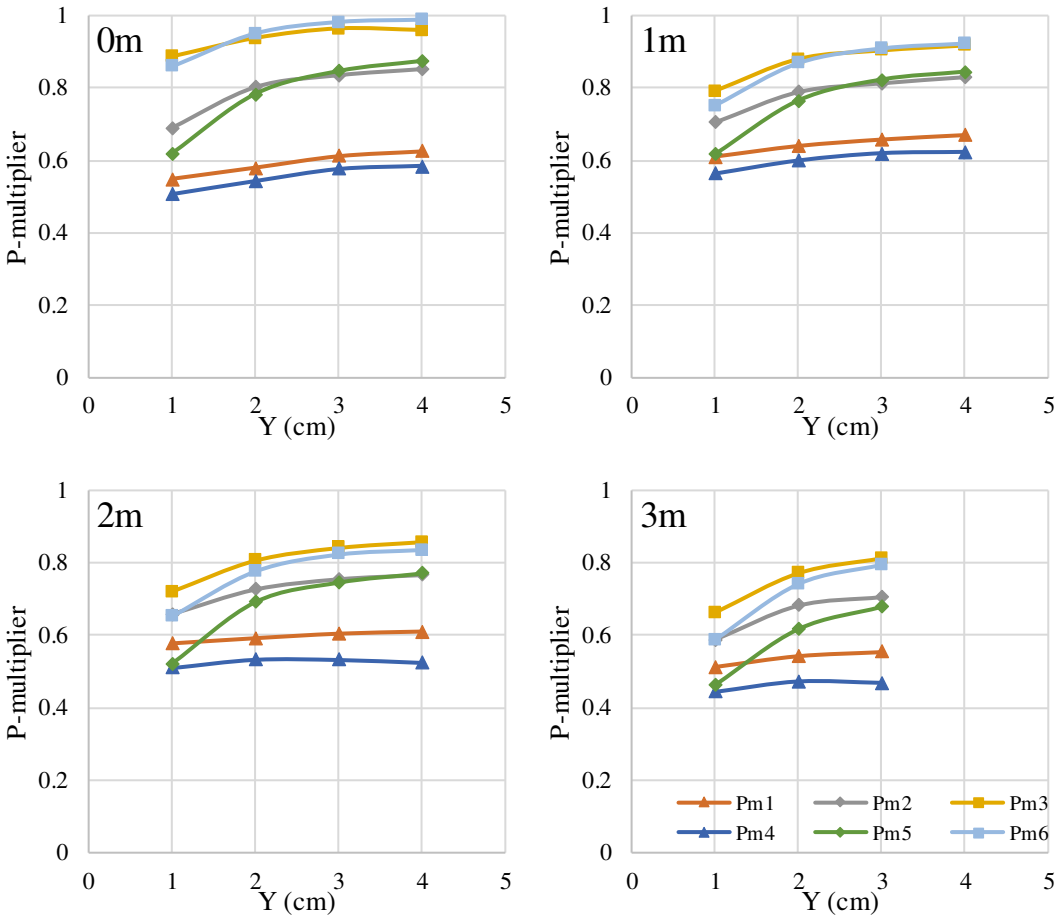


Figure 18. Variation of p-multipliers with lateral displacement for 3x3 pile group

4.3. Dynamic analysis results

Dynamic analyzes were performed using three different frequencies (1, 2 and 4Hz) and three different amplitudes (0.1, 0.3 and 0.5g) for single, 2x2 and 3x3 group piles. Thus, a total of 27 nonlinear dynamic analyzes were performed. The analysis is cumbersome because the model is large. High-capacity computers are needed for such analyzes. In the analyzes made, each single pile models take about 24 hours, while each 3x3 group pile models take approximately 48 hours with a high-performance computer of 32 cores.

Shear stress-strain behavior of static and dynamic analyses (2Hz and 0.5g) for a single pile is compared in Figure 19. The results of tie contact, in which the displacement and rotational degrees of freedom of the pile and the soil are equal, are also given in the figure. Since the system and loading are symmetric, soil nodes at the left and right side of the pile give similar results. Shear stress at the soil for tie contact seems to be much higher than the frictional

slip contact (labeled as "Int"). On the other hand, static analysis results are also higher than dynamic results under the same strain levels when the interaction is defined.

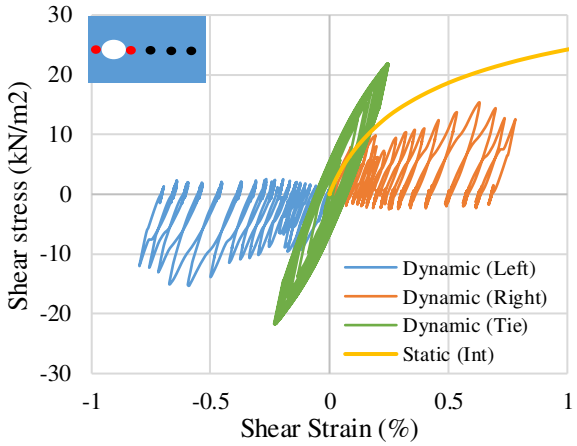


Figure 19. Comparison of shear stress-strain curves for single pile

The relative pile displacement is obtained by subtracting the pile displacement from the free field displacement (Yoo et al. 2013; Lim and Jeong 2018). On the other hand, free field displacement values should be taken from a distance greater than six times the pile diameter (6D) according to literature (see Figure 15). In this study, the free field displacement values were taken from a distance of approximately 14D to stay on the safe side. Moment-depth and relative displacement-depth relationships under 2Hz seismic loading for a single pile are compared in Figures 20 and 21, respectively. As the amplitude increases, the increase at the moment and displacement values are seen. This behavior is in line with the findings in the literature (Rovithis et al. 2009; Yoo et al. 2013). At small amplitudes, the moment changes the sign according to the loading direction, while the sign becomes the same as the amplitude increases. Static results are also given in the figures. Where the maximum displacements at the pile top are the same for the static and dynamic cases, while the displacement changes along the pile are close, there is a difference in the moment values.

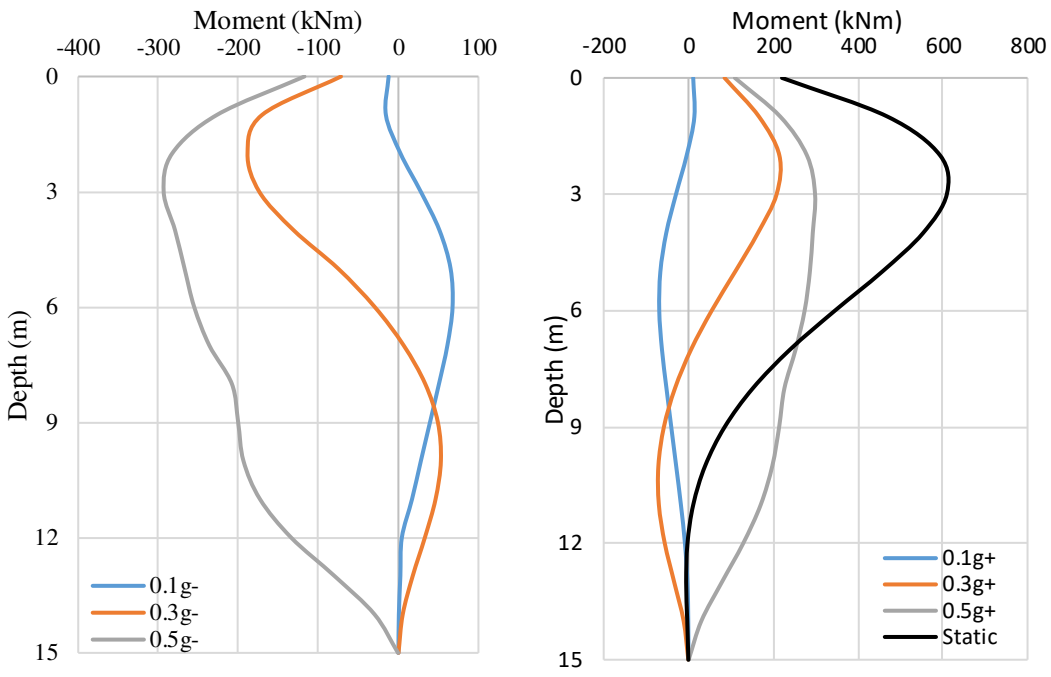


Figure 20. Comparison of moment-depth curves for different amplitudes (2Hz)

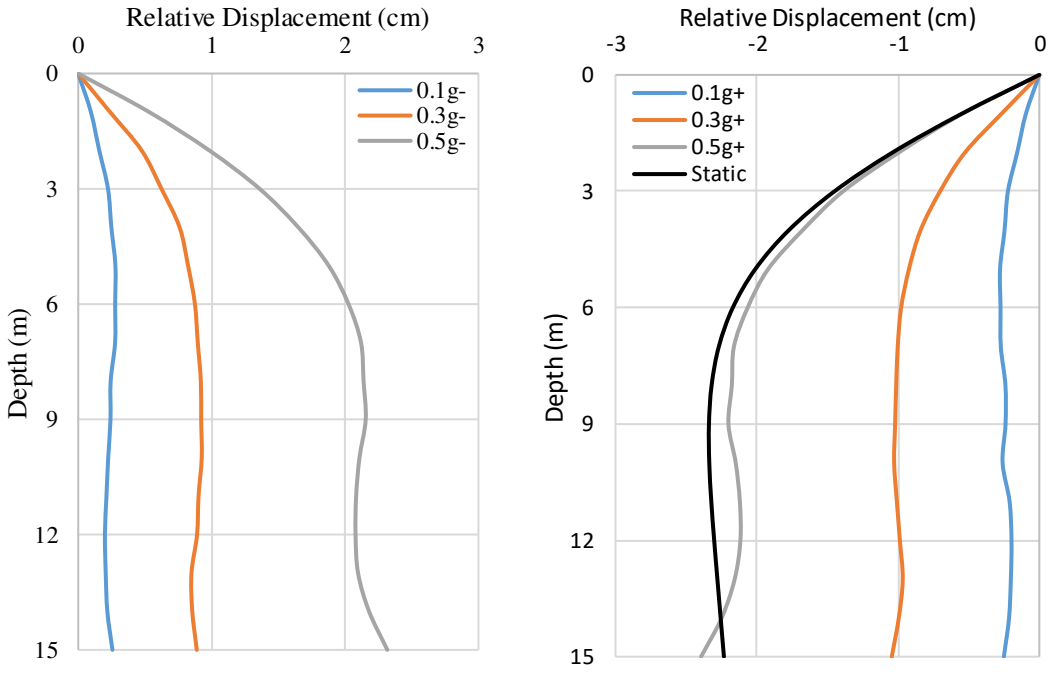


Figure 21. Comparison of displacement-depth curves for different amplitudes (2Hz)

Shear stress-strain behavior of soil node near pile 2 in static and dynamic analyses (2Hz and 0.5g) for 2x2 pile group are compared in Figure 22. It is seen that static and dynamic behavior are compatible with each other.

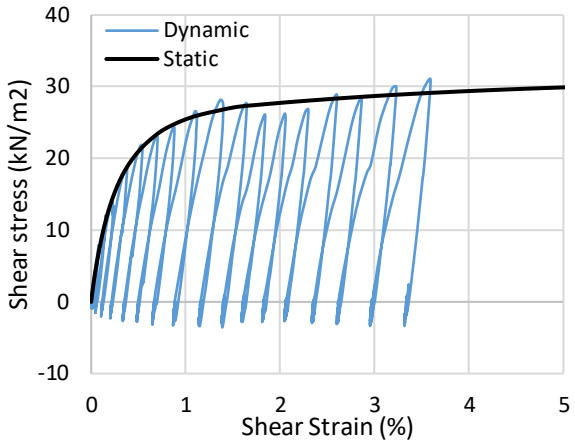


Figure 22. Shear stress-strain curve for 2x2 group pile

Moment-depth and relative displacement-depth relationships under 2Hz seismic loading for 2x2 group piles are compared in Figures 23 and 24, respectively. As indicated for single model results, the increase in amplitude increases the moments and displacements. The front piles take more moments in both loadings (+ or -) while experiencing less displacements. When both figures are examined, it can be seen that pile in the same row gives similar results due to symmetrical boundary conditions, meshes and loadings.

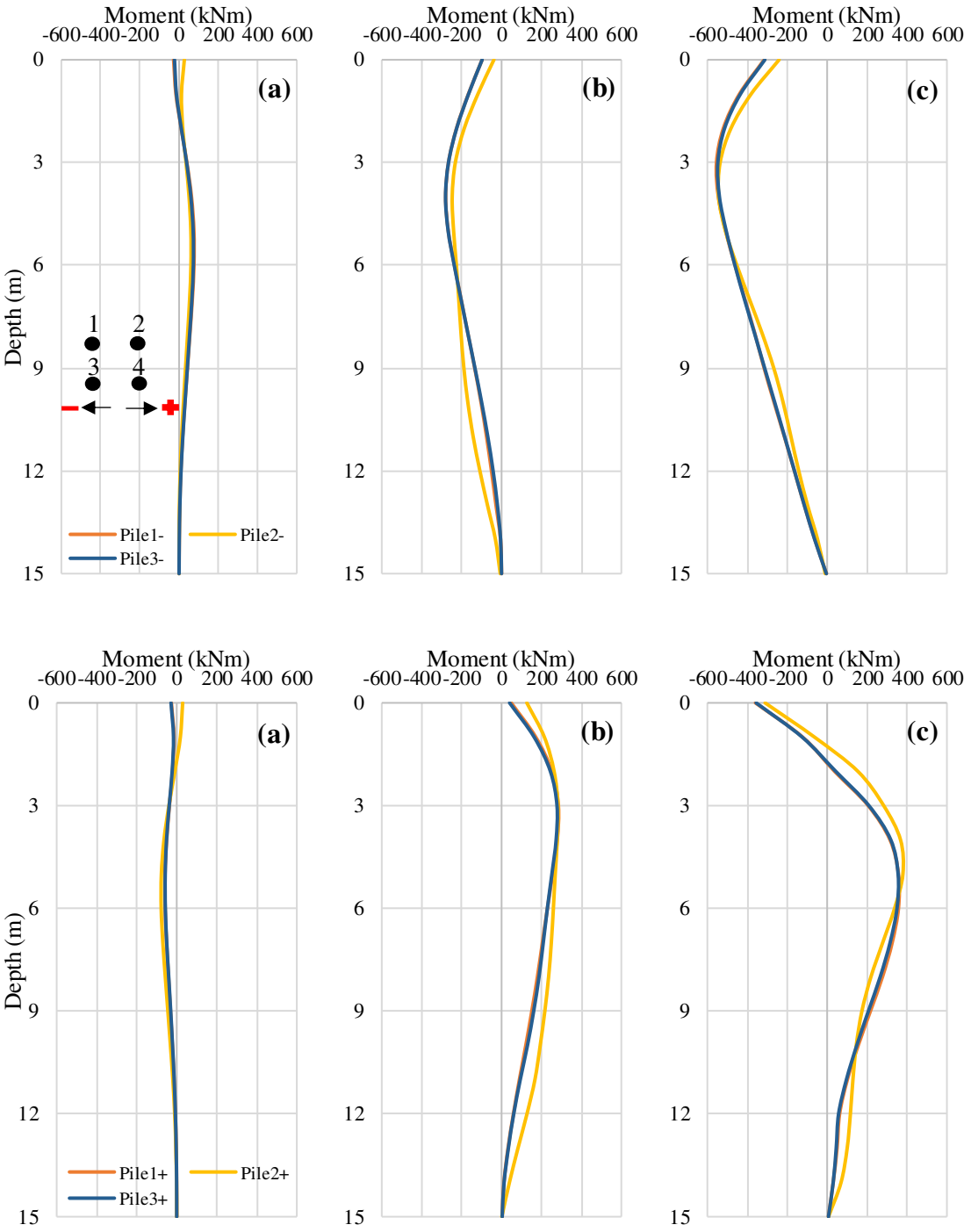


Figure 23. Moment-depth relationships for 2Hz: (a) 0.1g, (b) 0.3g and (c) 0.5g

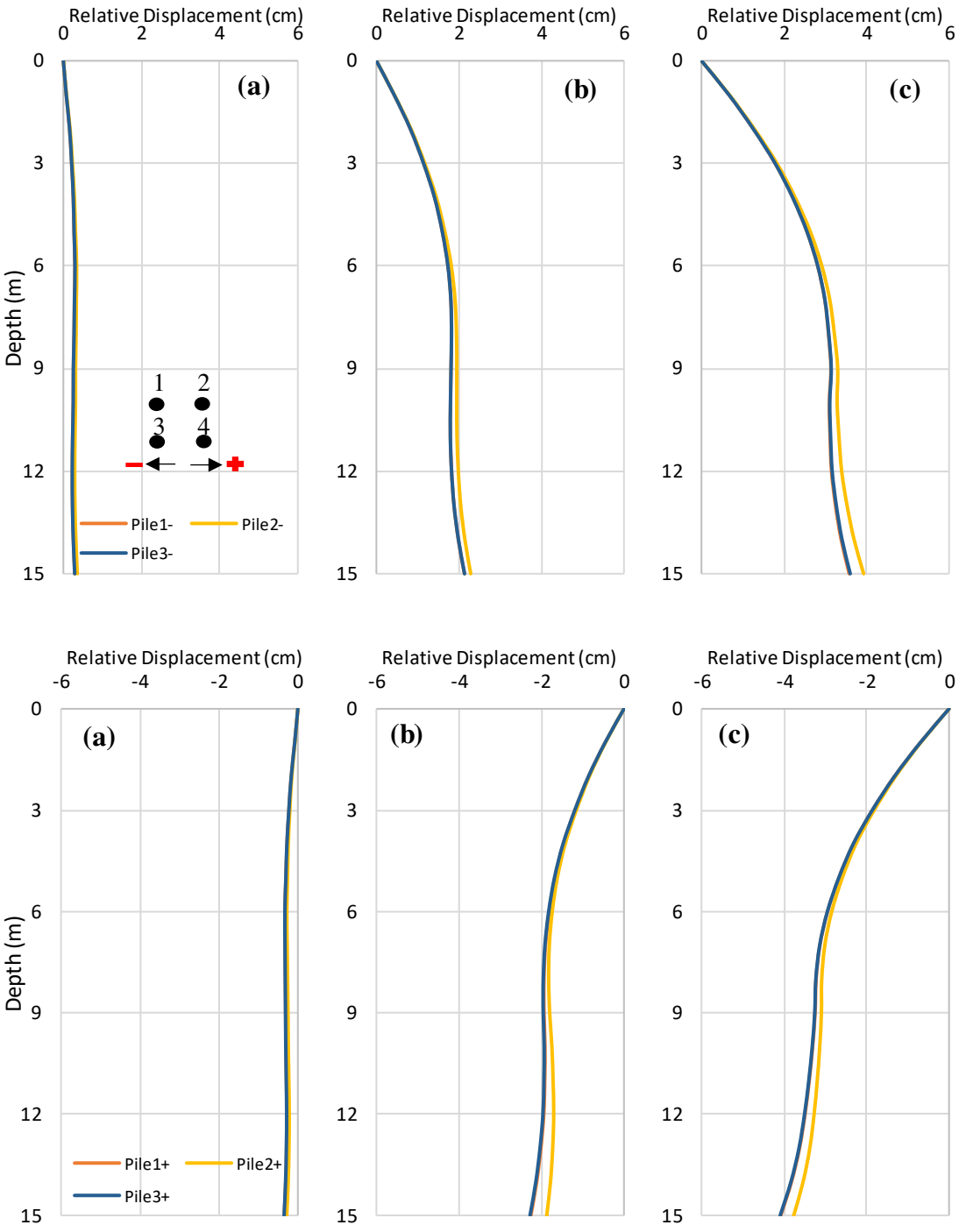


Figure 24. Displacement depth relationship for 2 Hz: (a) 0.1g, (b) 0.3g and (c) 0.5g

Shear stress-strain behavior of soil node near pile 3 in static and dynamic analyses (2Hz and 0.5g) for 3x3 pile group are compared in Figure 25. From the figure, it is clear that static results generate greater stresses than dynamic behavior.

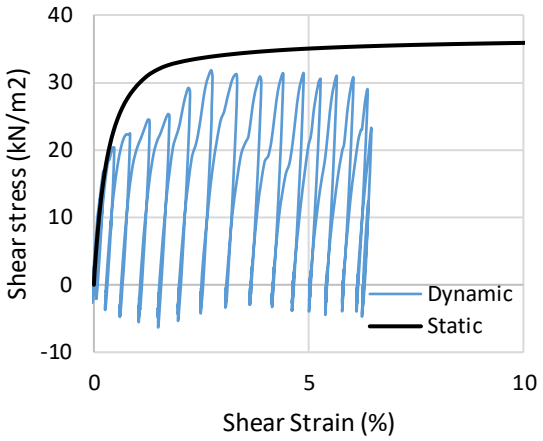


Figure 25. Shear stress-strain curve for 3x3 group pile

Moment-depth and relative displacement-depth relationships under 2Hz seismic loading for 3x3 group piles are compared in Figures 26 and 27, respectively. Considering the load distribution in the 3x3 group piles, it was concluded that the piles in the leading row received the highest load/moment at small amplitudes, but the piles in the middle row carried more load than those in the other rows at larger amplitudes. This is because there is an increase in strength in the soil around the middle row piles under dynamic loads. Here, there is a situation contrary to the load distribution obtained from the static analysis results in the literature and numerical results. According to studies in the literature, the piles in the front row receive the highest load, while the load decreases towards the rear rows. It has been understood that this result is different from the experimental results obtained from static horizontally loaded piles in the literature (Brown et al. 1988b; McVay et al. 1998; Ilyas et al. 2004). When Figure 27 is examined, it can be seen that pile in the same row (piles 1 and 7) gives similar results due to symmetrical boundary conditions, meshes and loadings.

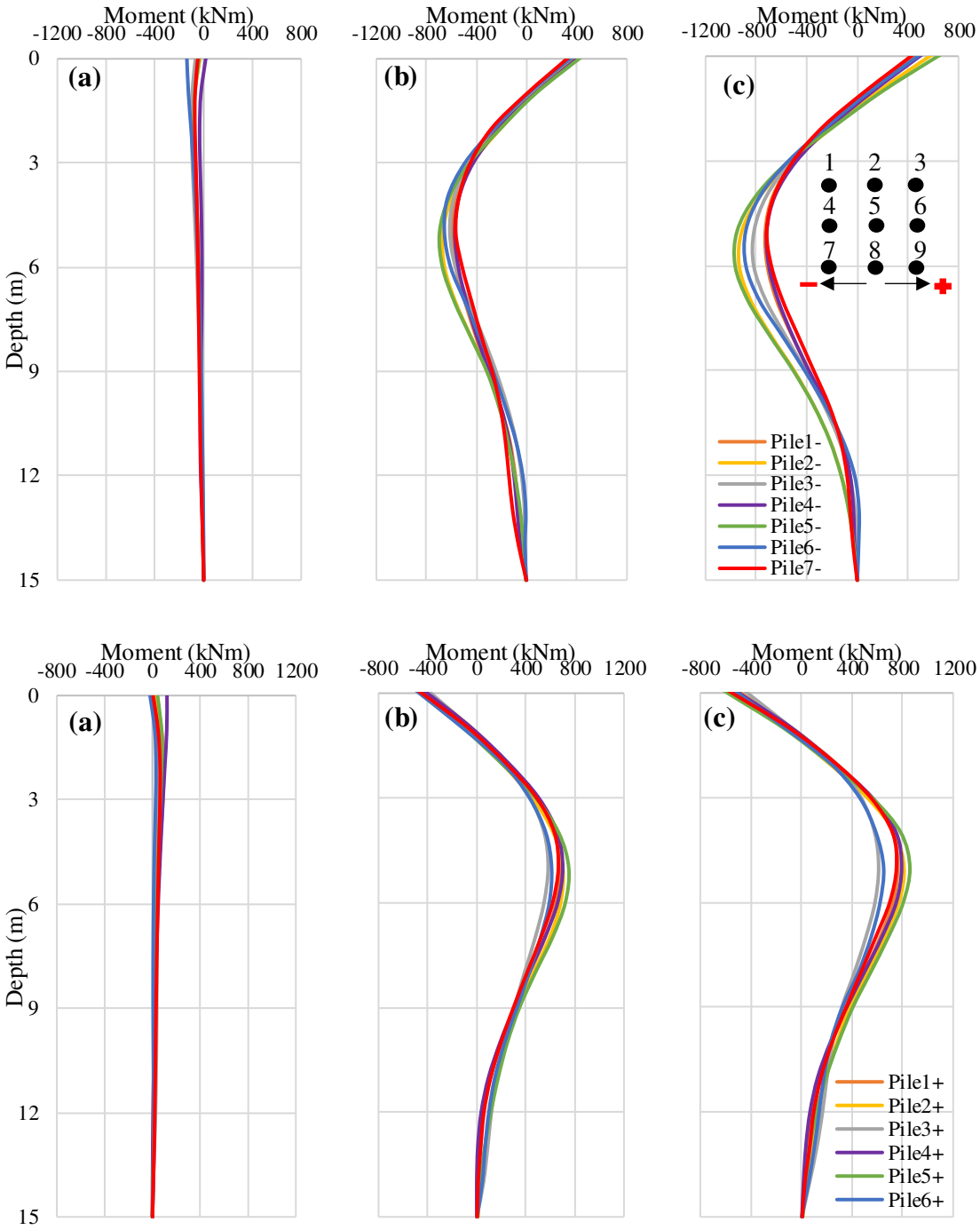


Figure 26. Moment-depth relationships for 2Hz: (a) 0.1g, (b) 0.3g and (c) 0.5g

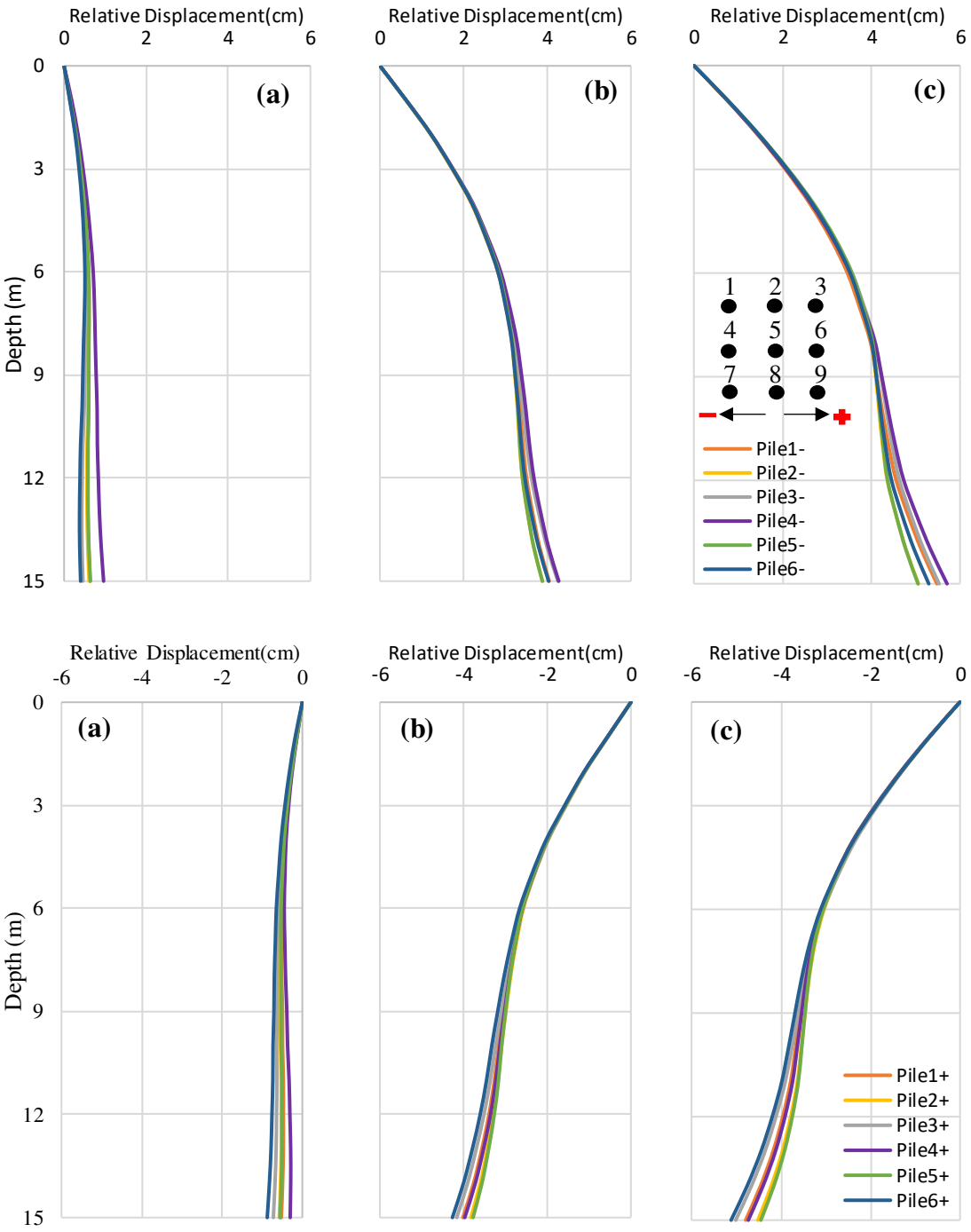


Figure 27. Displacement depth relationship for 2 Hz: (a) 0.1g, (b) 0.3g and (c) 0.5g

Soil resistance is expressed as the sum of the normal and shear/frictional resistances. The normal and shear forces occurring at 2m depth on the contact surface between the pile and the soil are shown in Figure 28. As expected, the normal contact forces increase in the middle of the pile and decrease towards the edges. Similarly, shear contact forces increase towards the edges and decrease towards the center.

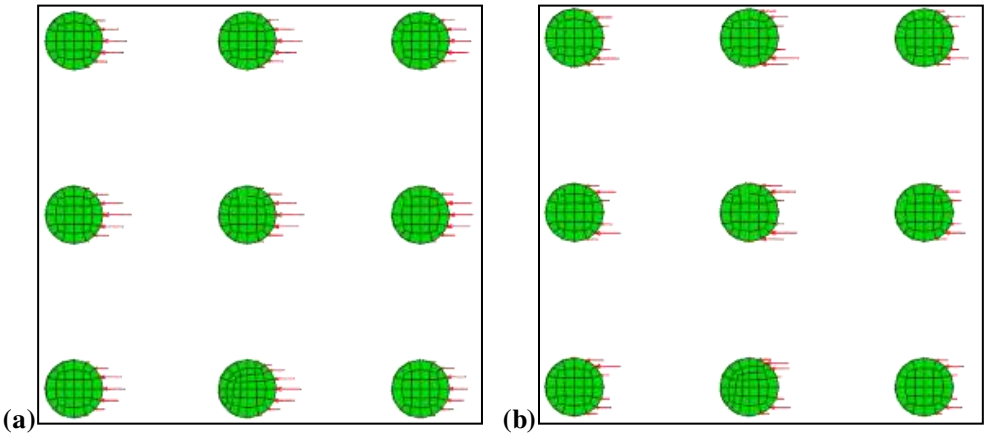


Figure 28. Forces on the surface of the piles at a depth of 2m (a) Normal contact and (b) Shear contact

4.4. Discussion on dynamic P-Y behavior

According to the Korean Society of Civil engineering (Korean society of civil engineering 2008), pile displacement must be at least 1% of the pile diameter to create p-y curves. For this reason, p-y curves were evaluated considering this criterion in the study. As explained in equation (6), soil resistance can be calculated from the pile nodes' normal and shear contact forces in contact with the soil elements.

Static and dynamic p-y curves for a single pile under 2Hz and 0.5g seismic loading are compared in Figure 29 for different depths. When the figures are scrutinized, it is seen that while the piles are moving in one direction, the resistance of soil in that direction increases. When the pile turns in the other direction, there is no resistance until it reaches the soil displaced in the previous cycle, but when the contact with the soil begins, the soil resistance starts to increase. When the pile changes direction, there is no contact and it is understood that the soil resistance approaches zero. This behavior reflects the actual soil-pile interaction in which separation, coupling and frictional behavior are defined. On the other hand, static p-y results are higher than dynamic results for each depth.

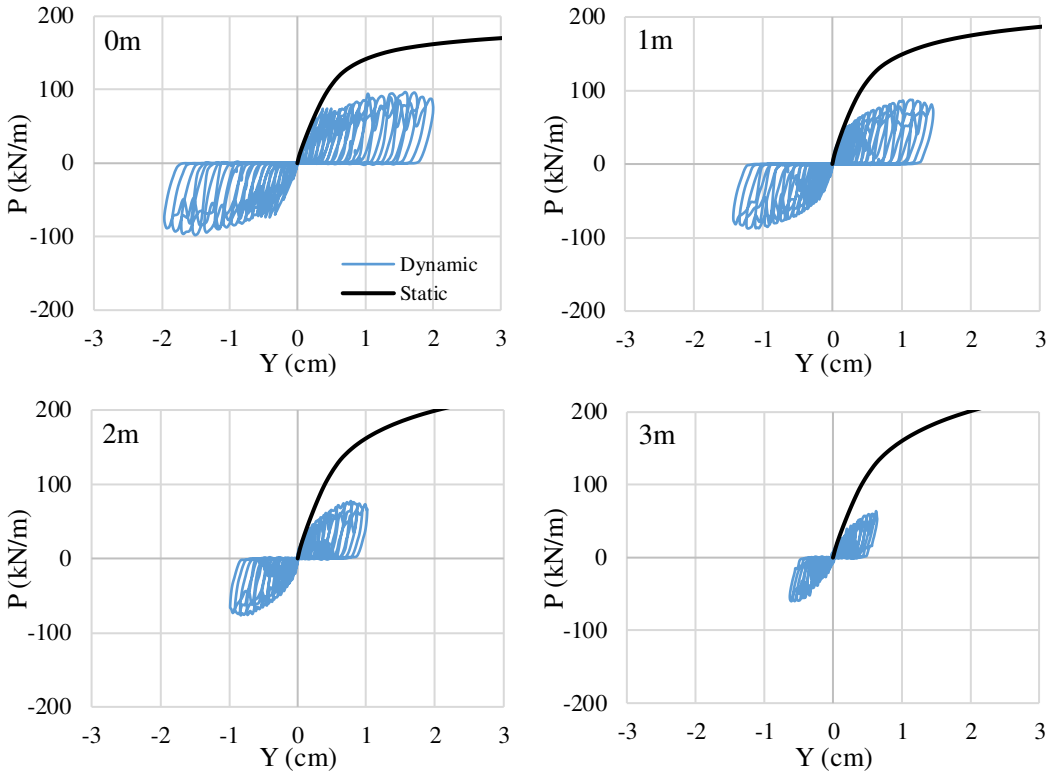


Figure 29. Comparison of static and dynamic p-y curves for single pile (2Hz-0.5g)

Static and dynamic p-y curves for pile 2 of 2x2 pile group under 2Hz and 0.5g seismic loading are compared in Figure 30 for different depths. Unlike single piles, peaks occur in the cyclic behavior of 2x2 group piles. This behavior is thought to be due to the well-known shadowing effect. Static and dynamic p-y curves for pile 3 of 3x3 pile group under 1Hz and 0.5g seismic loading are compared in Figure 31 for different depths. When the results of single, 2x2 and 3x3 group piles are evaluated together, it can be said that the behavior becomes more complex as the number of piles increases due to the shadowing effect.

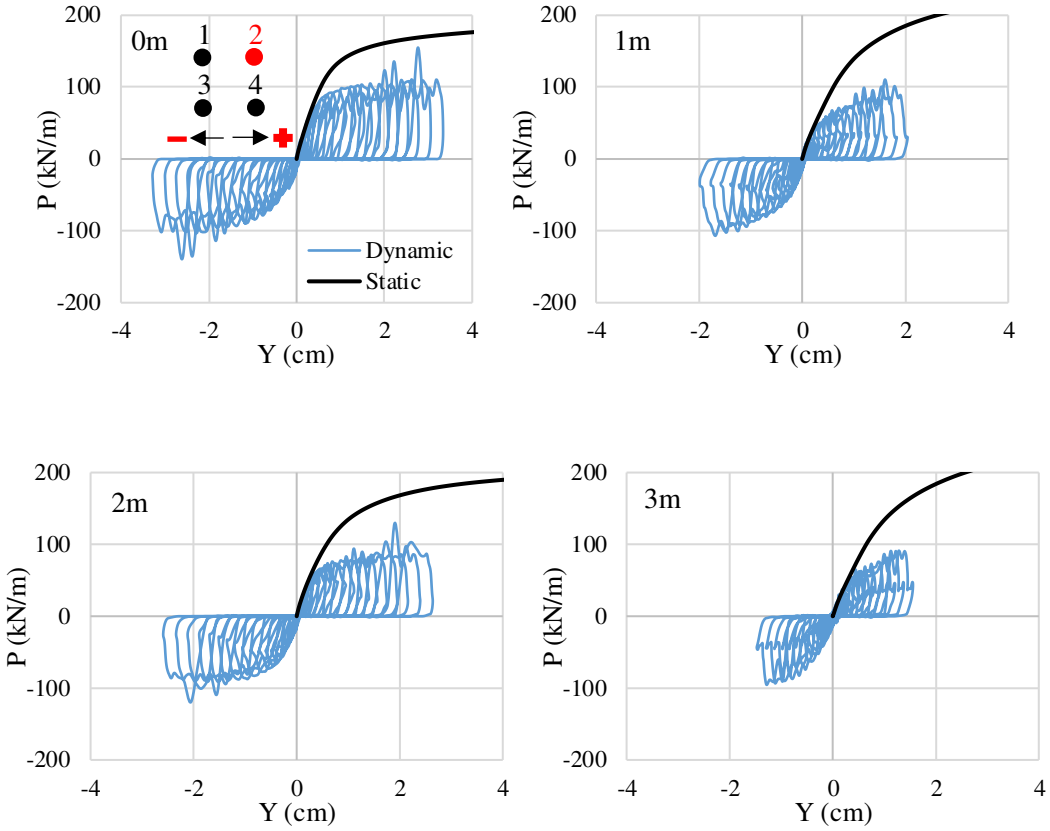


Figure 30. Comparison of static and dynamic p-y curves for pile 2 (2Hz-0.5g)

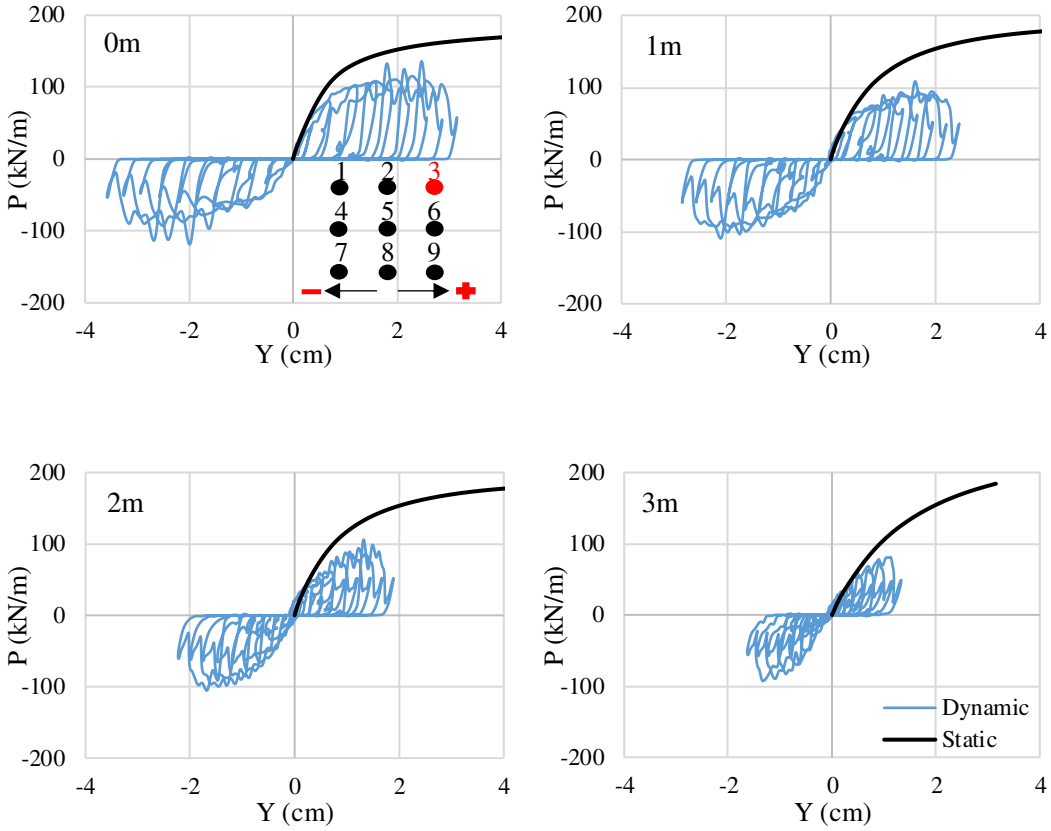


Figure 31. Comparison of static and dynamic p-y curves for pile 3 (1Hz-0.5g)

Figure 32 shows a single pile's static and dynamic p-y backbone curves under different frequencies for 1m and 2m depths in positive directions. The proposed curves obtained from API 2007 (API 2007) under cyclic loading is also added to the figure for comparison. It is stated in the literature (Yang et al. 2011; Yoo et al. 2013) that dynamic p-y backbone curves are obtained by combining the maximum displacements of increasing amplitude and the corresponding soil resistances. However, the backbone of cyclic p-y curves is used in the study because the load is given in an increasing amplitude. Since the pile has a displacement of less than 1% at the 4Hz frequency, the results of this frequency are not evaluated in the graphs. The results in Figure 32 indicate that the dynamic p-y curves are independent of frequency. This result is compatible with the experimental study available in the literature (Yoo et al. 2013). More importantly, although the dynamic curves are compatible with the static curves at small displacements, they are below the static curves at large displacements for any depths. The curves suggested by API seem to underestimate static results.

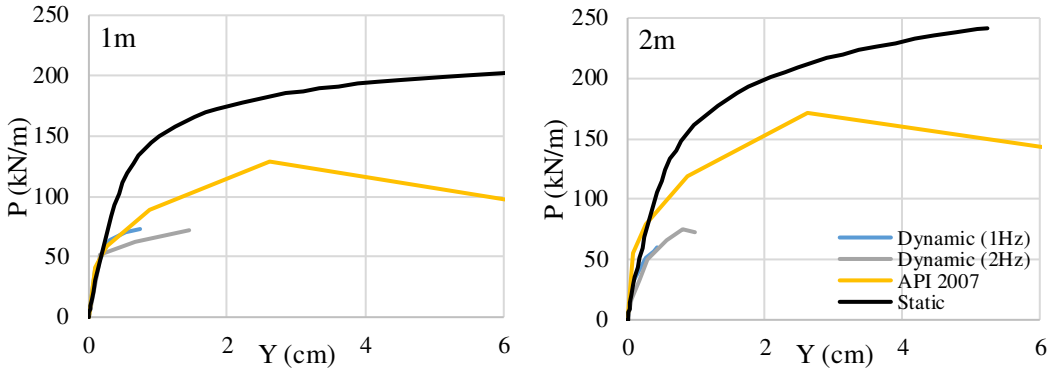


Figure 32. Comparison of p-y backbone curves for single pile

Figure 33 shows the static and dynamic p-y backbone curves of a 2x2 pile group under different frequencies for 1m and 2m depths in positive directions. As in single pile results, p-y curves are independent of frequency in 2x2 group piles. Similarly, dynamic curves fall under static p-y curves. API results in the figure are reduced by p-multipliers obtained from TBEC (TBEC 2018). Like single piles, API curves underestimate static results in 2x2 group piles.

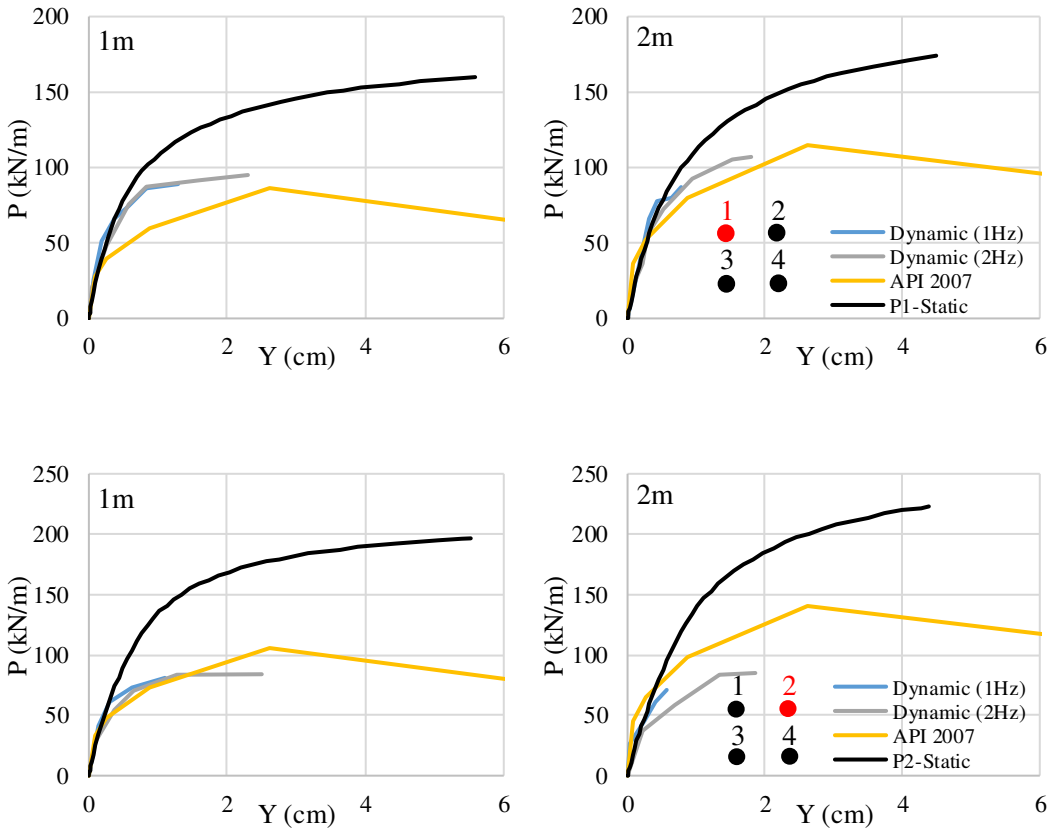
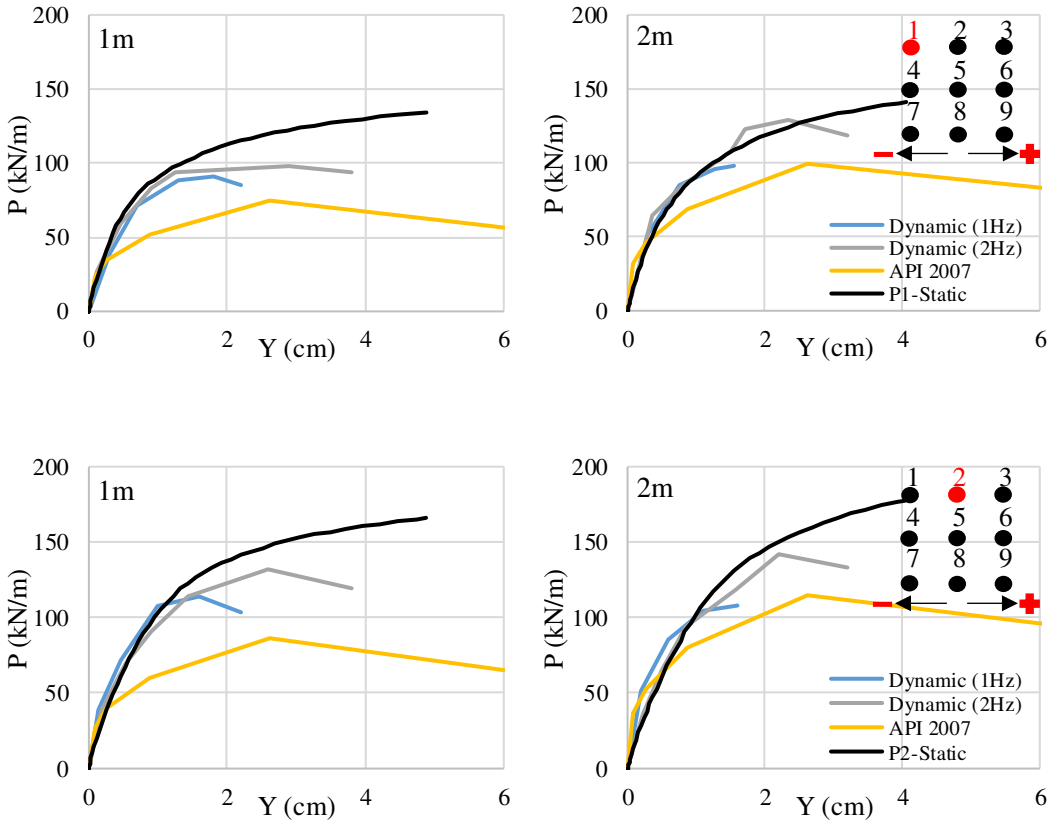


Figure 33. Comparison of p-y backbone curves for 2x2 group piles

Figure 34 shows the static and dynamic p-y backbone curves of a 3x3 pile group under different frequencies for 1m and 2m depths in positive directions. Similar to other results, p-y curves were independent of frequency in 3x3 group piles. Dynamic p-y curves stay under static ones at the leading row, although closer to static ones at the back rows. It is also evident that the API p-y curves underestimate the static results at deeper depths while an overestimation is encountered at shallow depths, as also found out by Li et al. (Li et al. 2017). The poor estimation of API curves is also emphasized in different studies (McGann et al. 2010; Rahmani et al. 2018)

Dynamic p-y backbone curves for 2x2 and 3x3 group piles are compared in Figures 35 and 36, respectively. According to the experimental and numerical static analysis results, while the piles in the leading row receive more load, the piles in the back row receive less load. According to the dynamic analysis of 2x2 group piles, as shown in Figure 35, p-y curves indicate that the soil resistance of piles at the back row (P1) is higher than that of the leading pile (P2). Similar to 2x2 group piles, soil resistance of piles at the middle row (P2) seems to be greater than leading (P3) and back rows (P1), as given in Figure 36. This is because there is an increase in soil resistance due to the compression in the soil around the middle row piles under dynamic loads. It has been understood that this result is different from the static experimental and numerical results obtained from horizontally loaded piles.



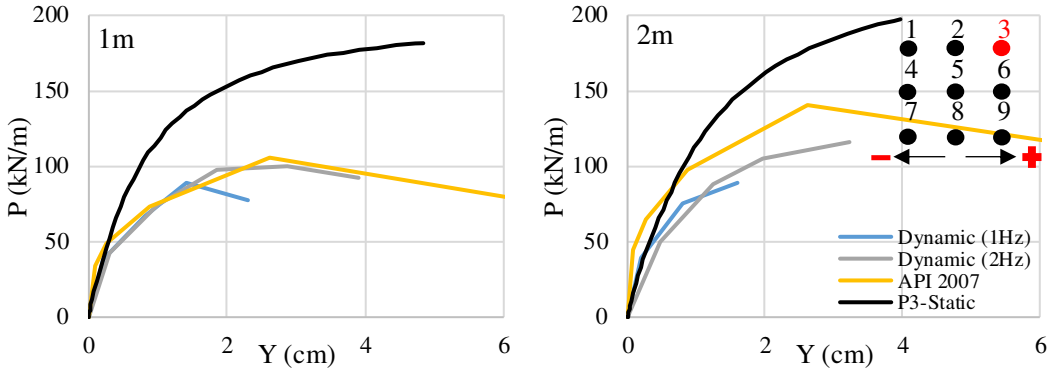


Figure 34. Comparison of p-y backbone curves for 3x3 group piles

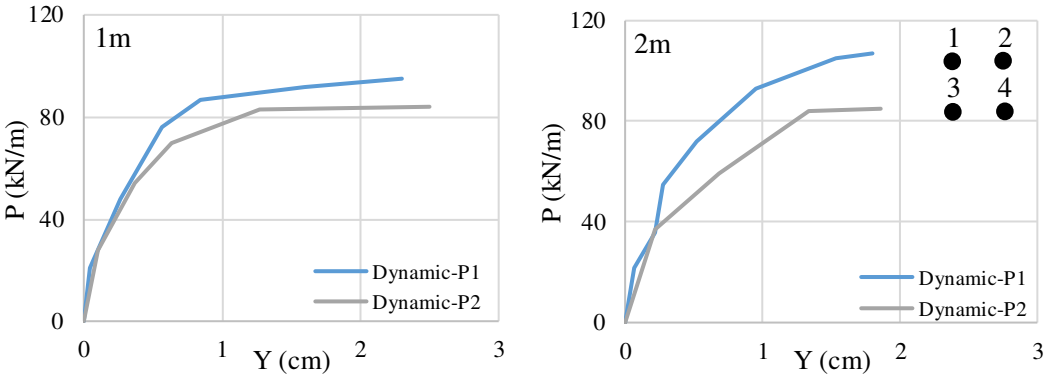


Figure 35. Comparison of dynamic p-y backbone curves for 2x2 group piles

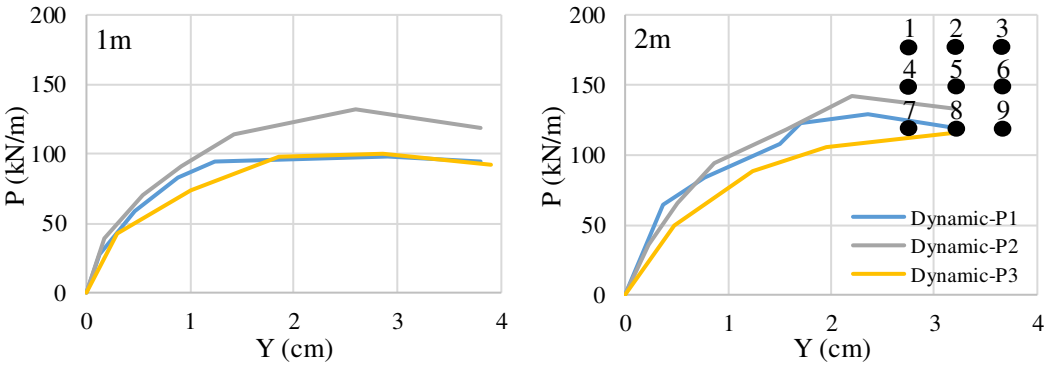


Figure 36. Comparison of dynamic p-y backbone curves for 3x3 group piles

5. Conclusions

This paper investigates the static and dynamic behavior of p-y curves and p-multipliers for group piles. For soil, the kinematic hardening model is used and its parameters are calibrated by the experimental study frequently used in the literature. For the dynamic analysis, non-reflecting infinite elements are applied at the boundaries.

The conclusions based on the analysis results and comparisons can be summarized as follows.

- Considering static analyses, as the number of piles increases, the depth at which the maximum moment, zero lateral displacements at the pile and the shear stress values at the soil around the pile increase.
- Static analyses on p-y curves confirmed that the pile at the front row carries more load than that of trailing rows, although more complex behavior is encountered under low displacement levels for both 2x2 and 3x3 group piles.
- P-multipliers are generated based on static numerical analyses for 2x2 and 3x3 group piles. The generated values seem to be compatible compared with the experimentally calculated ones. The p-multipliers are in a decreasing trend throughout pile depth.
- At low displacement levels, the p-multiplier value increases in the piles in the front and middle rows, while the p-multiplier starts to remain constant when the displacement increases. On the other hand, in the piles at the trailing rows, there is no significant change in the p-multiplier value while the displacement increases.
- Comparing the shear stress-strain behavior of static and dynamic analyses for a single pile, shear stress at the soil for tie contact seems much higher than the frictional slip contact. On the other hand, static analysis results are also higher than dynamic results under the same strain levels when the interaction is defined.
- In dynamic analyses of single, 2x2 and 3x3 group piles, as the amplitude of loading increases, the moment and displacement values increase both positively and negatively.
- The moments in the leading row in 2x2 group piles under dynamic loading are greater than the trailing row as in static analyses. However, in 3x3 group piles, the piles in the leading row received the highest load/moment at small amplitudes, but the piles in the middle row carried more load than those in the other rows at larger amplitudes. This is because there is an increase in strength in the soil around the middle row piles under dynamic loads. This load distribution contradicts the static load distribution of 3x3 group piles.

- Similar to moments, at lower amplitudes, the displacement profile of piles in the middle row is less than the piles behind and higher than the leading piles. However, the displacements of middle row piles at larger amplitudes seem smaller than other piles in the group.
- When static and dynamic P-Y curves are compared, it is understood that dynamic P-Y curves stay under static results for single pile, 2x2 and 3x3 group piles. On the other hand, API (2007) suggestions seem to underestimate the static P-Y backbone curves for single pile and all individual piles in groups.
- The dynamic P-Y backbone curves in clay are independent of frequency for all piles. Although the dynamic curves are compatible with the static curves at small displacements for single and 2x2 group piles, they are below the static curves at large displacements for any depths. Dynamic p-y curves for 3x3 group piles stay under static ones at the leading row, although they are closer to static ones at the back rows.
- Comparing the P-Y curves of the individual pile in 2x2 group piles, the soil resistance at the leading row piles is slightly greater than back row piles. However, in 3x3 group piles, the soil resistance of the piles in the middle row is greater than the leading row piles. This is because there is an increase in soil resistance due to the compression in the soil around the middle row piles under dynamic loads.

The conclusions drawn in the study are limited to the pile and soil parameters and soil material model used in the analyses. P-Y behaviors can also be compared with different material models to expand the scope of future studies.

Funding

The authors declare that no funds, grants, or other support were received during the preparation of this manuscript.

Competing Interests

The authors have no relevant financial or non-financial interests to disclose.

Author Contributions

All authors contributed to the study conception and design. Material preparation, data collection and analysis were performed by Mehmet Ömer Timurağaoğlu. The first draft of the manuscript was written by Mehmet Ömer Timurağaoğlu. All authors contributed writing - review and editing of the manuscript. All authors read and approved the final manuscript.

Data Availability

The datasets generated during and/or analysed during the current study are available from the corresponding author on reasonable request.

Acknowledgements

The authors greatly thank Bursa Uludag University for licensing of ABAQUS 2020 software.

References

AASHTO (2017) AASHTO LRFD bridge design specifications. Washington: American Association of State Highway and Transportation Officials.

Abaqus (2020) Documentation. Dassault Syst. Simulia Corp.

Adeel MB, Jan MA, Aaqib M, Park D (2020) Development of Simulation Based p-Multipliers for Laterally Loaded Pile Groups in Granular Soil Using 3D Nonlinear Finite Element Model. Appl Sci 11:26. https://doi.org/10.3390/app11010026

Anastasopoulos I, Gelagoti F, Kourkoulis R, Gazetas G (2011) Simplified constitutive model for simulation of cyclic response of shallow foundations: Validation against laboratory tests. J Geotech Geoenvironmental Eng 137:1154–1168. https://doi.org/10.1061/(ASCE)GT.1943-5606.0000534

API (2007) Recommended Practice for Planning, Designing and Constructing Fixed Offshore Platforms – Working Stress Design. API Publishing Services, American Petrolium Institute

Belinchon P, Sørensen KK, Christensen R (2016) A Case Study of the interaction between a pile and a soft soil focussing on negative skin friction using finite elment analysis. Proc 17th Nord Geotech Meet 513–522

Boulanger RW, Curras CJ, Kutter BL, et al (1999) Seismic Soil-Pile-Structure Interaction Experiments and Analyses. J Geotech Geoenvironmental Eng 125:750–759. https://doi.org/10.1061/(ASCE)1090-0241(1999)125:9(750)

Brown D, Morrison C, Reese LC (1988a) Lateral load behavior of pile group in sand. J Geotech Eng 114:1261–1276

Brown DA, Morrison C, Reese LC (1988b) Lateral load behaviour of pile group in sand. J Geotech Eng 114:1261–1276. https://doi.org/10.1016/0148-9062(89)92298-5

Chen WF, Mizuno E (1990) Nonlinear analysis in soil mechanics. (No. BOOK). Amsterdam: Elsevier

El Naggar MH, Bentley KJ (2000) Dynamic analysis for laterally loaded piles and dynamic p-y curves. Can Geotech J 1166–1183

Fatahi B, Van Nguyen Q, Xu R, Sun WJ (2018) Three-dimensional response of neighboring buildings sitting on pile foundations to seismic pounding. Int J Geomech 18:. https://doi.org/10.1061/(ASCE)GM.1943-5622.0001093

Gerolymos N, Gazetas G, Tazoh T (2005) Static and Dynamic Response of Yielding Pile in Nonlinear Soil. In: 1st Greece – Japan Workshop: Seismic Design, Observation, and Retrofit of Foundations. pp 25–36

Giannakos S, Gerolymos N, Gazetas G (2012) Cyclic lateral response of piles in dry sand: Finite element modeling and validation. Comput Geotech 44:116–131. https://doi.org/10.1016/j.compgeo.2012.03.013

Haouari H, Bouafia A (2020) A Centrifuge Modelling and Finite Element Analysis of Laterally Loaded Single Piles in Sand with Focus on P–Y Curves. Period Polytech Civ Eng 64:1064–1074. https://doi.org/10.3311/PPci.14472

Hashash YMA, Musgrove MI, Harmon JA, et al (2017) DEEPSOIL 7.0, User Manual

Ilyas T, Leung ; C F, Chow ; Y K, Budi SS (2004) Centrifuge Model Study of Laterally Loaded Pile Groups in Clay. J Geotech Geoenvironmental Eng 130:274–283. https://doi.org/10.1061/ASCE1090-02412004130:3274

Jeremić B, Jie G, Preisig M, Tafazzoli N (2009) Time domain simulation of soil-foundation-structure interaction in non-uniform soils. Earthq Eng Struct Dyn 38:699–718. https://doi.org/10.1002/EQE.896

Kampitsis AE, Giannakos S, Gerolymos N, Sapountzakis EJ (2015) Soil–pile interaction considering structural yielding: Numerical modeling and experimental validation. Eng Struct 99:319–333. https://doi.org/10.1016/j.engstruct.2015.05.004

Kim Y, Jeong S (2011) Analysis of soil resistance on laterally loaded piles based on 3D soil-pile interaction. Comput Geotech 38:248–257. https://doi.org/10.1016/j.compgeo.2010.12.001

Korean society of civil engineering (2008) Bridge design criteria. (In Korean)

Li W, Zhu B, Yang M (2017) Static Response of Monopile to Lateral Load in Overconsolidated Dense Sand. J Geotech Geoenvironmental Eng 143:04017026. https://doi.org/10.1061/(ASCE)GT.1943-5606.0001698
Lim H, Jeong S (2018) Simplified p-y curves under dynamic loading in dry sand. Soil Dyn Earthq Eng 113:101–111. https://doi.org/10.1016/j.soildyn.2018.05.017
Lu W, Zhang G (2020) New p-y curve model considering vertical loading for piles of offshore wind turbine in sand. Ocean Eng 203:107228. https://doi.org/10.1016/j.oceaneng.2020.107228
Lysmer J, Kuhlemayer RJ (1969) Finite dynamic model for infine media. J Eng Mech Div - Proc Am Soc Civ Eng 95:859–878
Mat Nor AH, Yahuda AH, Pakir F (2015) Analysis of Lightweight Concrete "Cakar Ayam" Foundation for Road Construction using Plaxis 3D Foundation Software. Appl Mech Mater 695:729–733. https://doi.org/10.4028/www.scientific.net/amm.695.729
Matlock H (1970) Correlations for design of laterally loaded piles in soft clay. In: Proceedings of the Annual Offshore Technology Conference. pp 1–18
McGann CR, Arduino P, Mackenzie-Helnwein P (2010) Applicability of Conventional p-y Relations to the Analysis of Piles in Laterally Spreading Soil. J Geotech Geoenvironmental Eng 137:557–567. https://doi.org/10.1061/(ASCE)GT.1943-5606.0000468
McVay M, Zhang L, Molnit T, Peter L (1998) Centrifuge Testing of Large Laterally Loaded Pile Groups in Sands. J Geotech Geoenvironmental Eng 124:1016–1026
Meimon Y, Baguelin F, Jezequel JF (1986) Pile group behaviour under long time lateral monotonic and cyclic loading. In: Proc. of Third International Conference on Numerical Methods in Offshore Piling. pp 285–302
Mucciacciaro M, Sica S (2018) Nonlinear soil and pile behaviour on kinematic bending response of flexible piles. Soil Dyn Earthq Eng 107:195–213. https://doi.org/10.1016/j.soildyn.2017.12.025
Nguyen Q Van, Fatahi B, Hokmabadi AS (2017) Influence of size and load-bearing mechanism of piles on seismic performance of buildings considering soil-pile-structure interaction. Int J Geomech 17:1–22. https://doi.org/10.1061/(ASCE)GM.1943-5622.0000869
Rahmani A, Taiebat M, Finn WDL, Ventura CE (2018) Evaluation of p-y springs for nonlinear static and seismic soil-pile interaction analysis under lateral loading. Soil Dyn Earthq Eng 115:438–447. https://doi.org/10.1016/J.SOILDYN.2018.07.049
Reese, Cox WR, Koop FD (1974) Analysis of Laterally Loaded Piles in Sand. Offshore Technology Conference, Texas
Reese LC, Cox WR, Koop FD (1975) Field Testing and Analysis of Laterally Loaded Piles in Stiff Clay. Offshore Technology Conference, Texas, pp 671–690
Reese, Wang ST, Arrellaga JA, et al (2019) GROUP: A program for the analysis of a group of piles subjected to vertical and lateral loading - User's manual
Reese, Welch RC (1975) Lateral loading of deep foundations in stiff clay. ASCE J Geotech Eng Div 101:633–649. https://doi.org/10.1016/0148-9062(75)90294-6
Rollins K, Olsen R, Egbert J, et al (2003) Response, analysis, and design of pile groups subjected to static & dynamic lateral loads (No. UT-03.03)
Rollins KM, Peterson KT, Weaver TJ (1998) Lateral Load Behavior of Full-Scale Pile Group in Clay. J Geotech Geoenvironmental Eng 124:468–478. https://doi.org/10.1061/(ASCE)1090-0241(1998)124:6(468)
Rovithis E, Kirtas E, Pitilakis K (2009) Experimental p-y loops for estimating seismic soil-pile interaction. Bull Earthq Eng 7:719–736. https://doi.org/10.1007/s10518-009-9116-7
TBEC (2018) Turkish Building Earthquake Code. Ankara, Turkey: Disaster and Emergency Management Authority (in Turkish)
Timurağaoğlu MÖ, Fahjan Y, Doğangün A (2021) P-Y curves for laterally loaded single piles: Numerical validation. Mar Georesources Geotechnol 1–9. https://doi.org/10.1080/1064119X.2021.1972063
Ting JM, Kauffman CR, Lovicsek M (1987) Centrifuge static and dynamic lateral pile behaviour. Can Geotech J 24:198–207. https://doi.org/10.1139/t87-025
Vucetic M, Dobry R (1991) Effect of soil plasticity on cyclic response. J Geotech Eng 117:89–107
Welch R, Reese L (1972) Lateral Load Behavior of Drilled Shafts. Res Rep Number 89-10 - Texas Highw Dep 1–231
Wolf JP (1985) Dynamic soil-structure interaction. Prentice Hall, Englewood Cliffs, New Jersey
Xiao-ling Z, Jing-jiu Z, Cheng-shun X (2020) A method for p-y curve based on Vesic expansion theory. Soil Dyn Earthq Eng 137:. https://doi.org/10.1016/J.SOILDYN.2020.106291
Yang EK, Choi JI, Kwon SY, Kim MM (2011) Development of dynamic p-y backbone curves for a single pile in dense sand by 1g shaking table tests. KSCE J Civ Eng 15:813–821. https://doi.org/10.1007/s12205-011-1113-0
Yang Z, Jeremic B (2003) Numerical study of group effects for pile groups in sands. Int J Numer Anal Methods Geomech 27:1255–1276. https://doi.org/10.1002/nag.321
Yoo M-T, Choi J-I, Han J-T, Kim M-M (2013) Dynamic P-Y Curves for Dry Sand from Centrifuge Tests. J

Earthq Eng 17:1082–1102. https://doi.org/10.1080/13632469.2013.801377
Zienkiewicz OC, Emson C, Bettess P (1983) A novel boundary infinite element. Int J Numer Methods Eng 19:393–404. https://doi.org/10.1002/nme.1620190307